**Bold black font: Topical editor and reviewer comments**
Black font: Author response

**Topical Editor Decision: Publish subject to technical corrections (23 Apr 2019) by Christoph Müller**
**Comments to the Author:**
**Dear Dr. Elshall and co-authors,**

**thank you for your thorough revision of the manuscript.**
**I'm happy to accept the paper for publication.**
**There are two typos that need quick attention: "peck" should be "peak" in line 680 (and the response) and "soil inspiration models" in line 751 should be "soil respiration models" I suppose?**

**Thanks for submitting to GMD**

**Christoph**

Thank you very much for handling the manuscript and for accepting to publish our work in GMD. We made the following minor corrections:

(1) We corrected the typos in line 680 and line 751
(2) We corrected a grammatical error is line 745: "understanding the conditions where accounting for auto-correlation can be achieved remain^" → "understanding the conditions where accounting for auto-correlation can be achieved remains"
(3) We changed the marker color of the efflux observations in Figure 2 from green to blue to make it consistent with the other figures in the manuscript.

# Bayesian Inference and Predictive Performance of Soil Respiration Models in the Presence of Model Discrepancy

Ahmed S. Elshall[1,2], Ming Ye[3,*], Guo-Yue Niu[4,5] and Greg A. Barron-Gafford[4,6]

[1] Department of Earth Sciences, University of Hawai'i Manoa, Honolulu, Hawaii, USA
[2] Water Resources Research Center, University of Hawai'i Manoa, Honolulu, Hawaii, USA
[3] Department of Earth, Ocean, and Atmospheric Science, Florida State University, Tallahassee, Florida, USA
[4] Biosphere 2, University of Arizona, Tucson, Arizona, USA
[5] Department of Hydrology and Water Resources, University of Arizona, Tucson, Arizona, USA
[6] School of Geography and Development, University of Arizona, Tucson, Arizona, USA

*Corresponding Author: Ming Ye, Telephone: (850) 644-4587, Email: mye@fsu.edu

Submitted for publication in Geoscientific Model Development

April, 2019

**Key Points**

(1) Bayesian inference and prediction are useful to evaluate multiple soil respiration models with different levels of model complexity.

(2) Data models used in Bayesian inference have substantial impacts on model parameter distributions and subsequently model predictions.

(3) Using exponential power distribution and considering heteroscedasticity in data models improve Bayesian inference and prediction.

Keywords: Soil respiration, modeling, Bayesian, likelihood function, data model, autocorrelation, heteroscedasticity, skew exponential power distribution, cross-validation, scoring rule

**Abstract**

Bayesian inference of microbial soil respiration models is often based on the assumptions that the residuals are independent (i.e. no temporal or spatial correlation), identically distributed (i.e. Gaussian noise) and with constant variance (i.e. homoscedastic). In the presence of model discrepancy, since no model is perfect, this study shows that these assumptions are generally invalid in soil respiration modeling such that residuals have high temporal correlation, an increasing variance with increasing magnitude of $CO_2$ efflux, and non-Gaussian distribution. Relaxing these three assumptions stepwise results in eight data models. Data models are the basis of formulating likelihood functions of Bayesian inference. This study presents a systematic and comprehensive investigation of the impacts of data model selection on Bayesian inference and predictive performance. We use three mechanistic soil respiration models with different levels of model fidelity (i.e. model discrepancy) with respect to number of carbon pools and explicit representations of soil moisture controls on carbon degradation, and accordingly have different levels of model complexity with respect to the number of model parameters. The study shows data models have substantial impacts on Bayesian inference and predictive performance of the soil respiration models such that: (i) the level of complexity of the best model is generally justified by the cross-validation results for different data models; (ii) not accounting for heteroscedasticity and autocorrelation might not necessarily result in biased parameter estimates or predictions, but will definitely underestimate uncertainty; (iii) using a non-Gaussian data model improves the parameter estimates and the predictive performance; and (iv) separate accounting for autocorrelation or joint inversion of correlation and heteroscedasticity can be problematic and requires special treatment. Although the conclusions of this study are empirical, the analysis may provide insights for selecting appropriate data models for soil respiration modeling.

## 1 Introduction

Developing accurate soil respiration models is important for realistic projection of global carbon [C] cycle, as global soils store 2,300Pg carbon, an amount more than 3 times that of the atmosphere (Schmidt et al., 2011) and release 60–75 Pg C/yr, about 7 times more $CO_2$ to the atmosphere than all human-caused emissions (Le Quéré et al., 2014). The major work on soil respiration modeling has been focused on advancing knowledge about model inputs and calibration data (e.g. Janssens et al., 2003; Peters et al., 2007; Scott et al., 2009; Barron-Gafford et al., 2011; Hilton et al., 2014) and on developing more advanced models for better representing soil microbial processes (e.g. Schimel and Weintraub, 2003; Allison et al., 2010; Davidson et al., 2011; Wieder et al., 2013, 2015; Xu et al., 2014; Zhang et al., 2014) . Integration of data and models is indispensable for improving predictability of the terrestrial carbon cycle, and statistical modeling is a vital tool for the model-data integration (Luo et al., 2011, 2014; Wieder et al., 2015). In addition, use of state-of-the-art statistical methods is necessary to accurately quantify uncertainty in parameters and structures of soil respiration models for improvement and practical uses of the models (Katz et al., 2013). A data model that is also known as a residuals model or an error model is used to characterize residuals (i.e., the difference between data and corresponding model simulations). While a large number of data models have been used (e.g. Elshall et al., 2018; Scholz et al., 2018) to our knowledge comprehensive and systematic evaluation of data models for soil respiration modeling has not been reported in literature.

The objectives of this study are to evaluate the impacts of data models on Bayesian inference and predictive performance of three mechanistic soil respiration models, and to use the evaluation results to make broader recommendations. The three models were developed by Zhang et al. (2014) to simulate the Birch effect (the peak soil microbial respiration pulses in response to episodic

118 rainfall pulses) at a site scale and a short temporal scale; understanding the Birch effect is important
119 for gaining mechanistic understanding of $CO_2$ efflux production (Högberg and Read, 2006; Vargas
120 et al., 2011). The models of Zhang et al. (2014) are based on an existing four-carbon pool model,
121 but have additional carbon pools and/or explicit representations of soil moisture controls on carbon
122 degradation and microbial uptake rates. The models were calibrated, and Bayesian model selection
123 was used to select the best model (Zhang et al., 2014). However, this effort was based on a single
124 data model. It is unknown whether the best model still remains the best (in terms of reproducing
125 the both calibration data and the cross-validation data) if a different data model is used. In addition,
126 since predictive performance of the models was not evaluated in Zhang et al. (2014), it is unknown
127 whether the best model will give the best predictions. These two questions are addressed in this
128 study by considering eight data models and by evaluating predictive performance in a manner of
129 cross-validation. The top two models (also the two most high fidelity models) ranked by Zhang et
130 al. (2014) are considered in this study, and the worst model (also the low fidelity model) is also
131 considered in this study for comparison. We use the terms model fidelity and model discrepancy
132 interchangeably. Model fidelity refers to the degree of realism of representing our scientific
133 knowledge with respect to the real world system. That is a high fidelity model has less discrepancy.
134 Evaluating predictive performance for the three models with different degrees of fidelity provides
135 more insights than a single model.

136 Bayesian inference in general uses the Bayes' theorem to update the prior distributions of
137 model parameters to posterior parameter distributions given a likelihood function of data. The
138 mathematical formulation of the (formal and informal) likelihood function requires a probabilistic
139 data model that however is intrinsically unknown due to unknown errors in all model components
140 such as model structures, parameters, and driving forces. Bayesian inference of soil respiration

models often adopts the assumption of independent, normally distributed and homoscedastic residuals (e.g. Ahrens et al., 2014; Bagnara et al., 2015, 2018; Barr et al., 2013; Barron-gafford et al., 2014; Braakhekke et al., 2014; Braswell et al., 2015; Correia et al., 2012; Du et al., 2015, 2017; Hararuk et al., 2014; Hashimoto et al., 2011; He et al., 2018; Klemedtsson et al., 2008; Menichetti et al., 2016; Raich et al., 2002; Ren et al., 2013; Richardson and Hollinger, 2005; Steinacher and Joos, 2016; Tucker et al., 2014; Tuomi et al., 2008; Xu et al., 2006; Yeluripati et al., 2009; Yuan et al., 2012, 2016; Zhang et al., 2014; Zhou et al., 2010). These assumptions are conveniently adopted to satisfy the requirement of using an unknown probability model in Bayesian statistics, which is called "a basic dilemma" by (Box and Tiao, 1992).

Postulating the data models is always based on assumptions about residual statistics, and the most widely used assumptions are paired as follows: (i) independent vs. correlated residuals, (ii) homoscedastic vs. heteroscedastic residuals, and (iii) Gaussian vs. non-Gaussian residuals. For soil respiration modeling few studies have relaxed the non-correlation assumption(e.g. Cable et al., 2008, 2011; Li et al., 2016b), the homoscedasticity assumption (e.g. Berryman et al., 2018; Elshall et al., 2018; Ogle et al., 2016; Tucker et al., 2013), and the non-Gaussian and homoscedasticity assumptions (e.g. Elshall et al., 2018; Ishikura et al., 2017; Kim et al., 2014). The recent study of Scholz et al. (2018) relaxed these three assumptions using the generalized likelihood function developed by Schoups and Vrugt (2010). However, few studies have focused on investigating appropriateness and impact of these assumptions for soil respiration modeling, by relaxing the independent residuals assumption ( Ricciuto et al., 2011) and the Gaussian residuals assumption (Ricciuto et al., 2011; van Wijk et al., 2008). By relaxing these three assumptions stepwise resulting in eight data models, to our knowledge this is the first study that systematically evaluates the impact of data model selection on Bayesian inference and predictive performance of soil

164 respiration modeling. In addition, to our knowledge this is the first soil respiration modeling study
165 that investigates the impact of data models in relation to model fidelity.

166 Relaxing these three assumption results in eight data models, which are shown in details in
167 Section 2. For example, combining the assumptions of independent, homoscedastic, and Gaussian
168 residuals leads to the standard least squares data model. This model is the simplest one among the
169 eight data models, since it requires only one parameter, i.e., the constant variance of the Gaussian
170 distribution. Note that there is a difference between the soil respiration model parameters and the
171 data model parameters. They technically can be jointly estimated, but one arises from assumptions
172 about soil respiration processes, and the other from assumptions about the residuals. Relaxing the
173 homoscedastic assumption to heteroscedastic gives the weighted least squares data model. It is
174 more complex because it has extra parameters to account for multiple variances for multiple data.
175 Whenever one or combinations of the three assumptions (independence, homoscedasticity, and
176 normality) are relaxed, the resulting data models become more complex and require more
177 parameters. Such systematic evaluation of data models (McInerney et al., 2017; Smith et al. 2010b,
178 2015) is necessary to evaluate appropriateness of residuals assumptions and their impacts on
179 Bayesian inference.

180 The assumptions of heteroscedastic, correlated, and non-Gaussian residuals are accounted for
181 by using the method of Schoups and Vrugt (2010) in the following procedure: (i) the correlation
182 is removed from the residuals by using an autoregressive model; (ii) the resulting residuals are
183 normalized by a linear model of variance; and (iii) the normalized residuals are characterized by
184 using the skew exponential power distribution. The data model parameters (i.e., coefficients of the
185 autoregressive model, the linear variance model, and the skew exponential power distribution) are
186 not specified by users, but estimated together with soil respiration model parameters during the

187 Bayesian inference. The skew exponential power distribution is general in that by adjusting the
188 values of its kurtosis and skewness parameters the distribution can produce other distributions such
189 as the Laplace distribution (van Wijk et al., 2008; Ricciuto et al., 2011) and other distributions
190 through using an exponential model with different kurtosis parameters (Tang and Zhuang, 2009).
191 It is worth pointing out that there exist other methods to account for the three assumptions. Evin
192 et al. (2013) suggested accounting for residual heteroscedasticity before accounting for residual
193 autocorrelation. Lu et al. (2013) developed an iterative two-stage procedure to separately estimate
194 physical model parameters and data model parameters. Evin et al. (2014) developed a similar
195 procedure to first estimate model parameters and then estimate heteroscedasticity and
196 autocorrelation parameters. While this study uses the method of Schoups and Vrugt (2010),
197 exploring other methods is warranted in future studies.

198 After investigating the impacts of the data models on Bayesian inference, this study evaluates
199 the impacts of the data models on predictive performance of the three soil respiration models.
200 Using random samples generated during the Bayesian inference, a prediction ensemble is produced
201 for each soil respiration model. The ensemble is used to evaluate predictive performance of the
202 models in a stochastic sense by estimating to what extent the models can predict future events. The
203 evaluation in this study is done in a cross-validation manner by splitting the dataset of $CO_2$ efflux
204 into two parts for Bayesian inference and cross-validation, respectively. The evaluation of
205 predictive performance is important because different data models may give different parameter
206 distributions and accordingly different predictive performance. For example, the study of van Wijk
207 et al. (2008) concluded that the choice of the residual function is crucial to achieve accurate model
208 prediction and parameter estimation. Shi et al. (2014) showed that the posterior parameter
209 distributions and predictive performance given by two data models (weighted least square and

skew exponential power distribution after removing heteroscedasticity and autocorrelation) are dramatically different, and a definitive conclusion was drawn that one data model is better than the other. The evaluation of predictive analysis is conducted for the following two cases: (1) the prediction ensemble is generated by random samples of the soil respiration models only (i.e. credible interval), and (2) the prediction ensemble is generated by random samples of not only the soil respiration models but also the data models (i.e. predictive interval). The two cases lead to different conclusions about the predictive performance. It is expected that the evaluation of predictive performance conducted in this study can help select the most appropriate data model to achieve optimal model predictions.

The remainder of the paper is organized as follows. Section 2 starts with a description of the evolving data models and their corresponding likelihood functions used in Bayesian inference, followed by a brief summary of the three soil respiration models. The results of Bayesian inference are discussed in Section 3 and Section 4, addressing the data model implications on parameter estimation and predictive performance, respectively. Section 5 summarizes the key findings and limitations of this study, and provides recommendations for approaching data model selection.

## 2 Methodology

This section starts with a description of the eight data models that account for the three pairs of assumptions about residuals in a stepwise manner in Section 2.1. The data models are used to build the likelihood functions used in Section 2.2 for Bayesian inference. The three soil respiration models and observations of $CO_2$ efflux are described in Sections 2.3 and 2.4, respectively. Metrics for evaluating predictive performance are presented in Section 2.5.

## 2.1 Data models

This study considers eight evolving data models starting from a data model that assumes independent, homoscedastic, and Gaussian residuals to a data model that relaxes all the three assumptions. The eight data models are based on the generic normalized residual,

$$a_t = \frac{\varepsilon_t}{\sigma_t} \qquad a_t \sim X\,, \tag{1}$$

where $\varepsilon_t = d_t - Y_t$ is the residual (the difference between data $d_t$ and its corresponding model simulation $Y_t$) at time or location $t$; $\sigma_t$ is the standard deviation of the residual; and $X$ is the probability density function (PDF) of $a_t$. The eight data models are formulated with different forms of $\varepsilon_t$, $\sigma_t$, and $X$. The standard least square (SLS) data model is

$$a_t = \frac{\varepsilon_t}{\sigma_0} \qquad a_t \sim N(0,1)\,, \tag{2}$$

where $\sigma_t = \sigma_0$ is a constant for all the data (i.e., homoscedasticity), and $X$ is the standard normal distribution, $N(0,1)$. The unknown parameter $\sigma_0$ is estimated jointly with unknown physical model parameters. If $\sigma_t$ is not a constant (i.e., heteroscedastic), SLS becomes the weighted least squared (WLS) data model. While heteroscedasticity can be accounted for through residuals transformation (e.g. Thiemann et al., 200; Smith et al., 2010b) or other similar approaches (Gragne et al., 2015) , a linear heteroscedastic model $\sigma_t = \sigma_0 + \sigma_1 Y_t$ is assumed here by following the studies of Thyer et al. (2009), Schoups and Vrugt (2010), and Evin et al. (2013, 2014). With the linear model, there is no need to estimate $\sigma_t$ for each data. Instead, $\sigma_t$ is calculated by estimating only two parameters, $\sigma_0$ and $\sigma_1$. The WSL data model is written as

$$a_t = \frac{\varepsilon_t}{\sigma_0 + \sigma_1 Y_t} \qquad a_t \sim N(0,1)\,. \tag{3}$$

The two unknown parameters $\sigma_0$ and $\sigma_1$ are estimated jointly with unknown physical model parameters. The linear model assigns smaller weight to the data with larger simulation, $Y_t$. If the simulation is small and $\sigma_0 \gg \sigma_1 Y_t$, the weight becomes constant for all data. Both SLS and WLS assume that $a_t$ is independently and identically distributed.

It is not uncommon that residuals are correlated in space and time, due to propagation of measurement errors (Tiedeman and Green, 2013) and model structure errors (Evin et al., 2014; Kavetski et al., 2013; Lu et al., 2013). The temporal correlation that occurs in the numerical example of this study can be accounted for by using a *p*-order autoregressive model. This leads to the data model of standard least square with autocorrelation (SLS-AC),

$$a_t = \frac{\varepsilon_t - \sum_{i=1}^{p} \phi_i \varepsilon_{t-i}}{\sigma_0} \qquad a_t \sim N(0,1) \tag{4}$$

where *p* is the order of autocorrelation, and $\phi_i$ is an autocorrelation coefficient. The unknown $\phi_i$ and $\sigma_0$ are estimated together with unknown model parameters. By extending the concept of correlated residuals to WLS leads to the weight least square with autocorrelation (WLS-AC),

$$a_t = \frac{\varepsilon_t - \sum_{i=1}^{p} \phi_i \varepsilon_{t-1}}{\sigma_0 + \sigma_1 Y_t} \qquad a_t \sim N(0,1) \tag{5}$$

The unknown parameters of $\sigma_0$, $\sigma_1$, and $\phi_i$ are estimated jointly with physical model parameters. Equations (2) – (5) assume that the residuals are Gaussian.

The next four data models are similar to the previous four models except that the standard normal distribution of $a_t$ is replaced by the skew exponential power distribution, $SEP(0,1,\xi,\beta)$, with zero mean and unit standard deviation (Schoups and Vrugt, 2010)

$$p(a_t \mid \xi, \beta) = \frac{2\sigma_\xi}{\xi + \xi^{-1}} \omega_\beta \exp\left[ -c_\beta \left| a_{\xi,t} \right|^{2/(1+\beta)} \right], \quad (6)$$

where $\xi$ is skewness, $\beta$ is kurtosis, $a_{\xi,t} = (\mu_\xi + \sigma_\xi a_t) \Big/ \xi^{sign(\mu_\xi + \sigma_\xi a_t)}$, $\mu_\xi = M(\xi - \xi^{-1})$,

$\omega_\beta = \dfrac{\Gamma^{1/2}[3(1+\beta)/2]}{(1+\beta)\Gamma^{3/2}[(1+\beta)/2]}$, $\sigma_\xi = \sqrt{(1 - M^2)(\zeta^2 + \zeta^{-2}) + 2M^2 - 1}$,

$M = \dfrac{\Gamma[1+\beta]}{\Gamma^{1/2}[3(1+\beta)/2]\Gamma^{1/2}[(1+\beta)/2]}$, and $c_\beta = \left( \dfrac{\Gamma[3(1+\beta)/2]}{\Gamma[(1+\beta)/2]} \right)^{1/(1+\beta)}$ are derived variables of $\beta$ and

$\xi$, and $\Gamma[.]$ is the gamma function. The kurtosis parameter $\{\beta \in \mathbb{R} : -1 \le \beta \le 1\}$ determines the peakness of the pdf such that the $\beta$ values of -1, 0, and 1 give uniform, Gaussian and Laplace distributions, respectively. The skewness parameter $\{\xi \in \mathbb{R} : 0.1 \le \xi \le 10\}$ determines the skewness of the pdf such that the $\xi$ values of 0.1, 1, and 10 give positively skewed, symmetric, and negatively skewed distributions, respectively. Setting $\beta = 0$ and $\xi = 1$ leads to $\mu_\xi = 0$, $\sigma_\xi = 1$, $\omega_\beta = 1/\sqrt{2\pi}$, $c_\beta = 1/2$ and $a_{\xi,t} = a_t$, and the skew exponential power distribution $SEP(0,1,\xi = 1, \beta = 0)$ becomes the standard normal distribution,

$$p(a_t \mid \xi = 1, \beta = 0) = \frac{1}{\sqrt{2\pi}} \exp\left[ -\frac{1}{2}(a_t)^2 \right]. \quad (7)$$

which is the data model of SLS in equation (2).

Replacing $a_t \sim N(0,1)$ with $a_t \sim SEP(0,1,\xi,\beta)$ in equations (2) – (5) leads to the data models SEP, WSEP, SEP-AC, and WSEP-AC as follows,

$$a_t = \frac{\varepsilon_t}{\sigma_0} \qquad a_t \sim SEP(0,1,\xi,\beta) \quad (8)$$

$$a_t = \frac{\varepsilon_t}{\sigma_0 + \sigma_1 Y_t} \qquad a_t \sim SEP(0,1,\xi,\beta). \quad (9)$$

$$a_t = \frac{\varepsilon_t - \sum_{i=1}^{p} \phi_i \varepsilon_{t-1}}{\sigma_0} \qquad a_t \sim SEP(0,1,\xi,\beta) \tag{10}$$

$$a_t = \frac{\varepsilon_t - \sum_{i=1}^{p} \phi_i \varepsilon_{t-1}}{\sigma_0 + \sigma_1 Y_t} \qquad a_t \sim SEP(0,1,\xi,\beta) \tag{11}$$

In comparison with the Gaussian data models, the SEP-based data models have two more parameters ( $\xi$ and $\beta$ ) to be estimated jointly with physical model parameters. Data model WSEP-AC, which is known as the generalized likelihood function, is the most commonly used SEP-based data model (e.g. Vrugt and Ter Braak, 2011; Hublart et al., 2016; Scholz et al., 2018). A summary table of the eight data models with corresponding parameters is provided in the supplementary materials.

## 2.2 Bayesian inference and likelihood functions

Consider a Bayesian inference problem for a nonlinear model, *f*, used to simulate state variables (e.g., $CO_2$ efflux), $\boldsymbol{d} = \boldsymbol{Y}(\boldsymbol{\theta}) + \boldsymbol{\varepsilon}$, where $\boldsymbol{d}$ is a vector of data, $\boldsymbol{\theta}$ is a vector of model parameters, and $\boldsymbol{\varepsilon}$ is a vector of residuals that may include errors in data, model parameters, and model structures. The goal of Bayesian inference is to estimate the posterior distributions, $p(\boldsymbol{\theta}|\boldsymbol{d})$, of model parameters, $\boldsymbol{\theta}$, given data, $\boldsymbol{d}$, using Bayes' theorem (Box and Tiao, 1992)

$$p(\boldsymbol{\theta} \mid \boldsymbol{d}) = \frac{p(\boldsymbol{d} \mid \boldsymbol{\theta})\, p(\boldsymbol{\theta})}{\int p(\boldsymbol{d} \mid \boldsymbol{\theta})\, p(\boldsymbol{\theta})\, d\boldsymbol{\theta}} \tag{12}$$

where $p(\boldsymbol{\theta})$ is the prior distribution, and $p(\boldsymbol{d}|\boldsymbol{\theta})$ is the likelihood function to measure goodness-of-fit between model simulations, $\boldsymbol{Y}(\boldsymbol{\theta})$, and data, $\boldsymbol{d}$. The prior distribution can be obtained from data of previous studies (e.g. Elshall and Tsai, 2014) or expert judgment. When prior information is lacking, a common practice is to assume uniform distributions with relatively large parameter ranges so that the prior distributions do not affect the estimation of posterior distributions.

The data models above can be used to construct the likelihood functions. For the Gaussian data models given in equations (2) – (5), the corresponding Gaussian likelihood functions are straightforward, and an example is equation (7). For the SEP data models, the corresponding likelihood that is called generalized likelihood function is (Schoups and Vrugt, 2010)

$$p(\boldsymbol{d}\,|\,\boldsymbol{\theta}) = p(\boldsymbol{\varepsilon}_t\,|\,\boldsymbol{\theta}) = \prod_{t=1}^{n} \sigma_t^{-1} \frac{2\sigma_\xi}{\xi+\xi^{-1}} \omega_\beta \exp\left(-c_\beta \left|a_{\xi,t}\right|^{2/(1+\beta)}\right). \tag{13}$$

where $n$ is the dimension of $\boldsymbol{d}$. The Gaussian likelihood functions are special case of the generalized likelihood functions. For example, by setting $\beta=0$, $\xi=1$, $\phi_i=0$, $\sigma_t=\sigma_0$, $\sigma_\xi=1$, $\mu_\xi=0$, $\omega_\beta=1/\sqrt{2\pi}$, $c_\beta=1/2$, and $a_{\xi,t}=a_t$, equation (13) becomes the likelihood function corresponding to the SLS data model. Replacing $\sigma_t=\sigma_0$ by $\sigma_t=\sigma_0+\sigma_1 E_t$, equation (13) becomes the likelihood function of the WLS data model.

In this study, the posterior distributions of the data model parameters are jointly estimated with the soil respiration model parameters using the MT-DREAM$_{(ZS)}$ code (Laloy and Vrugt, 2012). MT-DREAM$_{(ZS)}$ implements a Markov chain Monte Carlo (MCMC) algorithm by running multiple Markov chains in parallel with adaptive proposal distribution, multiple-try sampling, and sampling from an archive of past states. These state-of-the-art features assist in overcoming common challenges in the sampling space such as multimodality, ill-conditioning, and high dimensionality, and thus allow for accurate exploration of the targeted distributions.

### 2.3 Soil respiration models

Zhang et al. (2014) studied the Birch effect (the peak soil microbial respiration pulses in response to episodic rainfall pulses), and developed five models, evolving from an existing four-carbon pool model to models with additional carbon pools and/or explicit representations of soil moisture controls on carbon degradation and microbial uptake rates. Three of the five models are

used in this study, and they are dented as 4C, 5C, and 6C. Note that model 4C is model 4C_NOSM of Zhang et al. (2014), not their model 4C. Figure 1 is the diagram of model 6C, the most complex one among the five models. The simplest one, model 4C, has four carbon pools, i.e., soil organic carbon (SOC), dissolved organic carbon (DOC), microbial biomass (MIC), and enzymes (ENZ), and does not consider the soil moisture control on carbon degradation and microbial uptake rates. Models 5C and 6C have an explicit representation of soil moisture controls on the rates. Based on the dual Arrhenius and Michaelis–Menten kinetics model, the original SOC degradation rate, $V_{decom}$, is (Davidson et al., 2011; Davidson and Janssens, 2006)

$$V_{decom} = V_{\max} C_{ENZ} \frac{C_{SOC}}{K_m + C_{SOC}} \tag{14}$$

where $V_{\max}$ [$s^{-1}$] is the maximum SOC degradation rate per unit enzyme when the substrates is not limiting, $C_{ENZ}$ [$gCm^{-3}$] is enzyme pool size, $C_{SOC}$ [$gCm^{-3}$] is SOC pool size, and $K_m$ is the half-saturation for SOC. The original microbial uptake rate, $V_{uptake}$, is (Davidson et al., 2011; Davidson and Janssens, 2006)

$$V_{uptake} = V_{\max\_up} C_{MIC} \frac{C_{DOC}}{K_{m\_up} + C_{DOC}} \frac{C_{O2}}{K_{m\_upO2} + C_{O2}}, \tag{15}$$

where $V_{\max\_up}$ [$s^{-1}$] is the maximum DOC uptake rate when the substrates is not limiting, $C_{MIC}$ [$gCm^{-3}$] is the MIC pool size, $C_{DOC}$ [$gCm^{-3}$] is the DOC pool size, $C_{O2}$ [$m^3m^{-3}$] is the gas concentration of $O_2$ in the soil pore, and $K_{m\_up}$ [$gCm^{-3}$] and $K_{m\_upO2}$ [$m^3m^{-3}$] are the corresponding half-saturation constants for DOC and $O_2$, respectively. With the explicit representation of soil moisture control, the two rates become (Zhang et al., 2014)

$$V_{decom} = V_{\max} C_{ENZ} \frac{C_{SOC}}{K_m + C_{SOC}} \left( \frac{\theta}{\theta_s} \right) \tag{16}$$

$$V_{uptake} = V_{\max\_up} C_{MIC} \frac{C_{DOC}}{K_{m\_up} + C_{DOC}} \frac{C_{O2}}{K_{m\_upO2} + C_{O2}} \left( \frac{\theta}{\theta_s} \right) \quad (17)$$

where $\theta$ [-] is the volumetric soil moisture, and $\theta_s$ [-] is the porosity.

In addition to using the new rate equations, models 5C and 6C have more carbon pools. In model 5C, DOC is split into two sub-pools for wet zone and dry zone of soil pores, and only the wet DOC is used by MIC, as shown in Figure 1. The moisture-controlled microbial uptake rate becomes

$$V_{uptake} = V_{\max\_up} C_{MIC} \frac{C_{DOC\_w}}{K_{m\_up} + C_{DOC\_w}} \frac{C_{O2}}{K_{m\_upO2} + C_{O2}} \left( \frac{\theta}{\theta_s} \right). \quad (18)$$

where $C_{DOC\_w}$ [gCm$^{-3}$] is the DOC pool size in the wet soil pores. Model 6C is more complex in that ENZ is further split into two sub-pools for wet and dry pores, and both the wet and dry ENZ are subject to degradation, as shown in Figure 1. The moisture-controlled SOC degradation rate becomes

$$V_{decom} = V_{\max} C_{ENZ\_W} \frac{C_{SOC}}{K_m + C_{SOC}} \left( \frac{\theta}{\theta_s} \right) \quad (19)$$

for the wet ENZ and

$$V_{decom} = V_{\max} C_{ENZ\_D} \frac{C_{SOC}}{K_m + C_{SOC}} \left( 1 - \frac{\theta}{\theta_s} \right) \varepsilon_D \quad (20)$$

for the dry ENZ, where $C_{ENZ\_W}$ [gCm$^{-3}$] is the wet soil pores enzyme pool size, $C_{ENZ\_D}$ [gCm$^{-3}$] is the enzyme pool size in the dry soil pores, and $\varepsilon_D$ is the catalysis efficiency of the dry zone enzyme.

Due to considering the moisture control and adding more soil pools, model 5C is expected to be significantly better than model 4C for simulating the Birch effect. Since the accumulated ENZ in dry soil is secondary, model 6C is expected to be slightly better than model 5C. In terms of

model structural error, model 4C has the largest model structure error, model 5C has significantly less model structure error, and model 6C has the smallest model structural error. In other words, model 6C has the highest model fidelity (i.e. lowest model discrepancy) among the three models. As shown below, the degree of model structural error is reflected in the process of Bayesian inference and verified by the cross-validation.

### 2.4 Observations and parameter estimation

Figure 2 plots the time series of 17,016 observations of soil moisture and $CO_2$ efflux used in this study. The observations were obtained during the entire year of 2007, covering a long period of dry season prior to monsoon and episodic rainfall events during monsoon. The first two third of this dataset is used for the Bayesian inference, and the last one third is used for cross-validation. The inference and cross-validation periods have both dry and wet periods, as shown in Figure 2. The observation site is located within the Santa Rita Experimental Range (SRER, 31.8214°N, 110.8661°W, elevation 1,116 m) outside of Tucson, Arizona (Barron-Gafford et al., 2011; Scott et al., 2009). This savanna site was covered by 22% of perennial grass, forbs and subshrubs and 35% of mesquite. The soils are uniformly Comoro loamy sand (77.6% sand, 11.0% clay, and 11.4% silt). The half-hourly atmospheric forcing data were collected from measurements through an eddy covariance tower (Scott et al., 2009). This includes downward shortwave, longwave, precipitation, wind, air temperature, humidity, and pressure. Volumetric $CO_2$ concentration was measured at a half-hourly interval through compact probes. The $CO_2$ efflux was estimated from the gradient of $CO_2$ concentration measured at two depths of 2 cm and 10 cm through Fick's first law of diffusion, and the estimates were validated against measurements from a portable $CO_2$ gas analyzer.

391 The parameters estimated in this study include the parameters of the soil respiration models
392 (4C – 6C) and the parameters of the data models described in Section 2.1. The estimated
393 parameters of models 4C and 5C include the microbial carbon use efficiency (CUE) [g/g], enzyme
394 production rate, $k_e$ [g/m$^3$s], microbial turnover rate, $\tau_m$ [1/s], and enzyme turnover rate $\tau_e$ [1/s].
395 Uniform distributions are used as the prior in the Bayesian inference, and the ranges of the four
396 parameters are 0.2 – 1.00, $1\times10^{-12}$ – $1\times10^{-7}$, $1\times10^{-12}$ – $1\times10^{-5}$ and $1\times10^{-11}$ – $1\times10^{-6}$, respectively.
397 The values of other parameters are fixed at the values used in Allison et al. (2010). Model 6C has
398 two more parameters, and they are the catalysis efficiency $\varepsilon_D$ [-] and the turnover rate of the dry-
399 zone enzymes $\tau_{en}$ [1/s]. The prior of the two parameters are uniform distributions with the ranges
400 of 0.2 – 0.8 and $1\times10^{-12}$ – $1\times10^{-8}$, respectively.
401 The DREAM-based MCMC simulation is conducted for a total of 24 cases, the combinations
402 of eight data models and three soil respiration models. For each case, the parameter distributions
403 are obtained after drawing a total of $5\times10^5$ samples using five Markov chains. The Gelman and
404 Rubin (1992) R-statistic is used for convergence diagnostic, and it approaches one in less than
405 40,000 samples. The initial 50% of the samples are discarded during the burn-in period.

406 **2.5 Metrics for evaluating predictive performance**

407 Three criteria are used to evaluate the predictive performance of the soil respiration models
408 and data models, and they are central mean tendency, dispersion, and reliability. Each criterion is
409 measured by a single metric. In addition, a newly defined metric by (Elshall et al., 2018) is also
410 used for simultaneously measuring the three criteria.
411 The central mean tendency is measured in this study using the Nash-Sutcliffe model efficiency
412 (NSME) coefficient (Nash and Sutcliffe, 1970),

413 $$NSME = 1 - \sum_{i=1}^{n} (d_i - \overline{\mathbf{Y}_i})^2 \Big/ \sum_{i=1}^{n} (d_i - \overline{\mathbf{d}})^2 , \quad (21)$$

where $n$ is the number of cross-validation data, $d_i$ is the $i$-th data, $\bar{\mathbf{d}}$ is the mean of the data, and $\overline{\mathbf{Y}_i}$ is the mean of the prediction ensemble, $\boldsymbol{Y}_i$, for $d_i$. NSME ranges from -∞ to 1, with $NSME = 1$ corresponding to a perfect match between data and mean prediction, i.e., the ensemble is centered on the data. $NSME = 0$ indicates that the model predictions are as only accurate as the mean of the data, while an efficiency $NSME < 1$ indicates that the mean of data is a better prediction than the mean prediction.

In addition to the central mean tendency, it is also desirable that the ensemble is precise with small dispersion and reliable to cover all the data. This study uses a nonparametric metric for dispersion, and it is the sharpness of a prediction interval (e.g. Smith et al., 2010a)

$$Sharpness = 1/n \sum_{i=1}^{n} \left[ Max(\mathbf{Y}_i) - \mathrm{Min}(\mathbf{Y}_i) \right] \tag{22}$$

where $\mathbf{Y}_i$ is the prediction ensemble within the 95% prediction interval, the Bayesian credible interval, not the confidence interval used in nonlinear regression (Lu et al., 2013). Smaller values of sharpness indicate better prediction precision. Reliability is measured using predictive coverage. (e.g. Hoeting et al., 1999), which is the percentages of data contained in the prediction interval. Larger predictive coverage values are preferred.

To account for the trade-off between the three metrics, Elshall et al. (2018) defined relative model score (RMS) that simultaneously measure all the three criteria. Scoring rules are commonly used in hydrology to assess predictive performance (e.g., Weijs et al., 2010; Westerberg et al., 2011). RMS is used in this study to measure the relative predictive performance of the combinations of soil respiration models and data models. For combination $M_j$, RMS is defined as

$$RMS(M_j) = \sum_{i=1}^{n} \frac{p(d_i \mid \mathbf{Y}_{ij}, M_j)}{\sum_{j=1}^{m} p(d_i \mid \mathbf{Y}_{ij}, M_j)} \times 100 \quad (23)$$

where $m$ is the number of combinations; the ensemble prediction $\boldsymbol{Y}_{ij}$ is similar to $\boldsymbol{Y}_i$ above with index $i$ over time and index $j$ specific to the $j$-th combination. The density function $p(d_i|\boldsymbol{Y}_{ij})$ can be evaluated by first obtaining the density function $p(\boldsymbol{Y}_{ij})$ of the ensemble prediction $\boldsymbol{Y}_{ij}$ (e.g., by using the kernel density function) and then evaluating $p(d_i|\boldsymbol{Y}_{ij})$ using interpolation methods based on the intersection of $\boldsymbol{Y}_{ij}$ and $d_i$. More details about evaluating *RMS* can be found in Elshall et al. (2018). This evaluation is based purely on the model predictions, and does not involve any assumptions on the models, their parameters, and likelihood functions. Larger RMS values indicate better overall predictive performance. A figure of our workflow scheme is presented in the supplementary materials.

## 3 Results of Bayesian Inverse Modeling

This section analyzes the residuals of the best realization (with the highest likelihood value) of the MCMC simulation to understand whether the assumptions of the eight data models hold. The impacts of the data models on the posterior parameter distributions are also analyzed.

### 3.1 Residual characterization

Figure 3 shows residual plots for model 6C based on data models SLS and WSEP-AC. SLS is the simplest data model with the assumptions of homoscedastic, independent, and Gaussian residuals, and the WSEP-AC is the most complex one without the assumptions. Model 6C is the most complex model and also the best one as ranked by Zhang et al. (2014) using Bayesian model selection. The variable $a_t$ plotted in Figures 3a-3c and Figures 3d-3f is defined in equations (2) and (11), respectively. Figures 3a – 3c show that all the three residual assumptions are violated when SLS is used, because (i) the residual variance is not constant, but increases as a function of the

simulated $CO_2$ efflux (Figure 3a); (ii) the autocorrelation function at most lags is beyond the 95% confidence interval (Figure 3b); (iii) the standard normal density function cannot adequately characterize the residuals (Figure 3c). Figures 3d-f show that, after relaxing the three assumptions, the processed residuals, $a_t$, can be well characterized by WSEP-AC. Figure 3d shows that, after normalizing $\varepsilon_t$ with the linear variance ( $\sigma_t = 0.034 + 0.099 E_t$ ), the variation of the variance of $a_t$ becomes significantly smaller, although the variance is still not constant. Figure 3e shows that, after removing a first-order autoregressive model from $\varepsilon_t$, $a_t$ becomes less correlated, although the correlation is not fully removed. The two coefficients of the autoregressive model are $\phi_1 = 0.989$ and $\phi_2 = 4.5\times10^{-6}$; the small value of $\phi_2$ indicates that there is no need to attempt an autoregressive model of higher order. Figure 3f shows that $a_t$ follows the SEP distribution with the estimated skewness coefficient of $\xi = 0.933$ and kurtosis coefficient of $\beta = 0.998$. As a summary, Figure 3 shows that it is important to examine the residuals and to determine whether the selected data model is adequate for charactering the residuals. Although WSEP-AC still cannot perfectly characterize $\varepsilon_t$, it is significantly better than SLS.

Although the Gaussian assumption used in SLS is violated for model 6C (Figure 3c), this is not generally the case for other data models and soil respiration models. This is shown in Figure 4, which presents the quantile-quantile (Q-Q) plot for the eight data models and the three soil respiration models. For SLS, WLS, SLS-AC, and WLS-AC, the theoretical quantiles are based on the standard normal distribution, $N(0,1)$; for SEP, WSEP, SEP-AC, and WSEP-AC, the theoretical quantiles are based on the standard skew exponential power distribution, $SEP(0,1,1,0)$. If the residuals follow the assumed standard distributions, the Q-Q plots fall on the 1:1 lines, marked as the theoretical lines in Figure 4. If the residuals are Gaussian or SEP but not standard, the Q-Q plots fall on a straight line but not the 1:1 line. Figures 4a and 4e show that, for all the soil

479 respiration models, the Q-Q plots of SLS and SEP deviate significantly from the theoretical lines
480 and exhibit fat-tail behaviors, which is an indication of outliers (Thyer et al., 2009). The deviation
481 is reduced after accounting for autocorrelation in SLS-AC and SEP-AC, as shown in Figures 4c
482 and 4g. It is interesting to observe from the two figures that the Q-Q plots of the three models are
483 almost visually identical. The deviation is almost fully removed after accounting for
484 heteroscedasticity in WLS and WSEP in that their corresponding Q-Q plots fall on the 1:1 lines,
485 especially for models 5C and 6C, as shown in Figures 4b and 4f. However, the Q-Q plots start
486 deviating from the 1:1 lines as shown in Figures 4d and 4h, after accounting for both
487 heteroscedasticity and autocorrelation in WLS-AC and WSEP-AC. As a summary, Figure 4 shows
488 that, for the numerical example of this study, either the Gaussian or the SEP distribution is valid if
489 heteroscedasticity is accounted for in the data models. However, accounting for autocorrelation in
490 the data models does not help improve the characterization of the residual distributions.

491 **3.2 Posterior parameter distributions**

492 While Figures 3 and 4 help understand validity of the three assumptions used in the data
493 models, the impacts of the data models on estimating model parameter distributions must be
494 evaluated separately. This section discusses the impact of the data model selection on parameter
495 estimation with the objective of understanding whether incorrect specification of the data model
496 necessarily leads to biased parameter estimates. Such assessment is not a trivial task for two main
497 reasons. First, microbial soil respiration models aggregate complex natural processes and spatial
498 details into simpler conceptual representations. As a results several model parameters are effective
499 values of several complex natural processes that cannot be actually measured in the field as
500 discussed by Vrugt et al. (2013). In addition, even for model parameter that can be measured in
501 the field, since the model structure is imperfect, calibrated parameter values are sometimes beyond

their physically reasonable range, as discussed by Pappenberger and Beven (2006). This is often undesirable, if we seek to make the models more mechanistically descriptive.

We focus our discussion on carbon use efficiency (CUE) for microbial growth due to two reasons: (1) CUE is a fundamental parameter in microbial soil respiration models, and (2) a physically reasonable range for CUE can estimated. The concept of microbial CUE(Allison et al., 2010; Bradford et al., 2008; Manzoni et al., 2012; Wieder et al., 2013) has been used to present fundamental microbial processes in recent microbial enzyme models (Allison et al., 2010; German et al., 2011; Schimel and Weintraub, 2003; Wang et al., 2013). The microbial CUE, which is marked between MIC and CO2 in Figure 1, controls microbial growth, enzyme production and microbial respiration. A physically reasonable range of CUE can be estimated from the physical viewpoint (Tang and Riley, 2014). Sinsabaugh et al. (2013) showed that the thermodynamic calculations support a maximum CUE of 0.60 and that previous studies that estimate CUE in terrestrial systems report a mean value of 0.55. Theoretically, there is no lower limit for CUE as it can approach zero, and CUE$<$ 0.1 has been reported for terrestrial ecosystems (e.g., Fernández-Martínez et al., 2014) and used in modeling studies (Li et al., 2014). Note that, for inverse modeling with MCMC sampling, we did not assume CUE maximum value of 0.6. In other words, for parameter estimation and predictive performance we did not impose the constraint that CUE is less than 0.6. We merely use this CUE maximum value of 0.6 to evaluate whether the posterior CUE parameter samples obtained using different data models and different soil respiration models are within the physically reasonable range of 0 ~ 0.6.

Figure 5 plots the CUE posterior marginal density of the three soil respiration models obtained using the eight data models. The physical range between zero and 0.6 is marked in yellow. Figure 5 shows that the CUE posterior parameter distribution of Model 6C obtained using the data models

525 that does not account for autocorrelation are within the physically reasonable range. For models
526 4C and 5C, the posterior parameter samples are outside the range for six data models. For model
527 4C, the posterior parameters are within the physical range only for data models SEP and WSEP;
528 for model 5C, the two data models are WLS and WSEP. It is not surprising to find the posterior
529 parameter distribution of models 4C and 5C, which have a certain degree of model structure error,
530 to be out of the physically plausible range. This can be attributed to two reasons. First, the model
531 solution can be biased toward the missing processes in the model structure such as the additional
532 carbon pool in both 4C and 5C or missing the explicit accounting for soil moisture in 4C. Second,
533 biased parameter estimation can compensate for model structure inadequacy and other sources of
534 discrepancy in both the physical models and the data models.

535 In addition, it is important to understand how accounting for autocorrelation, heteroscedasticity
536 and non-Gaussian residuals can affect the parameter estimation. First, it is observed in Figure 5e-
537 h that biased parameter estimates are outside the physically reasonable range when autocorrelation
538 is explicitly accounted for. This may suggest again that accounting for heteroscedasticity is
539 desirable but accounting for autocorrelation is not. A possible reason is that filtering
540 autocorrelation may reduce the residual space such that the transformed residual space cannot
541 correspond to the parameter space of the models. In other words, parameter information may be
542 lost due to filtering out autocorrelation. However, it is not fully understood why this does not occur
543 for the model 6C under data model SLS-AC (Figure 5e), and more research is warranted. Second,
544 unlike accounting for auto-correlation, accounting only for heteroscedasticity (i.e., WLS and
545 WSEP) only amplifies or reduces the variance without affecting the structure of the residual space.
546 Figures 5c-d show that account for heteroscedasticity (i.e. WLS and WSEP) tends to improve the
547 parameter estimation in comparison with homoscedastic data models (i.e., SLS and SEP) shown

548 in Figure 5a-b. Finally, with respect to non-Gaussian residuals, Schoups and Vrugt (2010)
549 suggested that, compared to Gaussian pdf, the peaked pdf of the SEP with a longer tail is useful
550 for making parameter inference robust against outliers. To a certain degree, this can be
551 substantiated by the results in Figure 5a-d, in that SEP and WSEP provide more favorable
552 parameter estimates than SLS and WLS.

553 Finally, Figure 5a shows that the posterior parameter distributions of SLS are very narrow for
554 the three soil respiration models. The narrow distributions can be attributed to several reasons.
555 Since SEP distribution can have longer tails than Gaussian distribution, this can further increase
556 the samples acceptance ratio from tails resulting in wider distribution (Figure 5b). In addition,
557 accounting for heteroscedasticity will result in wider posterior parameter distribution (Figure 5c)
558 due to accepting higher variances at peak effluxes. Moreover, filtering correlation (Figure 5e-h)
559 increases the entropy, and leads to wider distributions.

560 **4. Results of Predictive Performance**

561 Based on the last one third of the $CO_2$ efflux observations, a cross-validation test was
562 conducted for the combinations of three soil respiration models and eight data models. For the
563 cross-validation period, the predictive performance is examined using the four statistical metrics
564 that are defined in Section 2.5. The metrics are also calculated for the calibration period. This is
565 not to perform Bayesian model selection given the calibration data, but to better understand the
566 impact of data models on predictive performance of the three soil respiration models. For each
567 calibration and each cross-validation data, a prediction ensemble is generated from the two
568 perspectives of parametric uncertainty only and total uncertainty, as presented in Section 4.1 and
569 4.2, respectively.

570

571 **4.1 Predictive performance with parametric uncertainty of soil respiration model**

572 In this section the ensemble is generated by running the soil respiration models with the
573 posterior samples (obtained from the Bayesian inference) of the physical model parameters. In
574 other words, the ensemble addresses parametric uncertainty of the soil respiration models only.
575 Considering the relative contribution of parametric uncertainty only will provide insights for
576 modeling approaches that attempt to segregate various sources of uncertainty (e.g., Thyer et al.,
577 2009 ; Tsai and Elshall, 2013). The four statistics above (i.e. NSME, sharpness, coverage, and
578 RMS) are calculated for the three soil respiration models and the eight data models. Taking data
579 models SLS and WSEP-AC as an example, Figure 6 plots the data (for the calibration and cross-
580 validation periods separately) along with the mean and 95% credible intervals of the prediction
581 ensemble for the three models.

582 Figure 6 shows that the data models affect model simulations for all the models. The statistics,
583 especially RMS, indicate that WSEP-AC has better predictive performance than SLS. This is most
584 visually obvious for model 6C during the cross-validation period after 330 days, as the prediction
585 ensemble of SLS (Figure 6k) cannot cover the observations, whereas the prediction ensemble of
586 WSEP-AC can (Figure 6l). This conclusion that WSEP-AC outperforms SLS agrees with that
587 drawn from Figures 3 and 4.

588 Figure 7 plots the four statistics for all the soil respiration models and data models. Figures 7a
589 and 7b show the predictive performance with respect to the central mean tendency measured by
590 NSME for both the calibration and cross-validation periods respectively. The results indicate that,
591 under all data models, the low fidelity model 4C over-fits the data and results in biased predictions,
592 in that the NSME values become significantly worse (e.g., from 0.6 to -0.6) from the calibration
593 to the cross-validation period. This is confirmed by the visual inspection of Figures 6a and 6g for

data model SLS and of Figures 6b and 6h for data model WSEP-AC. For models 5C and 6C, their NSME values vary with the data models; and the central mean accuracy is the worst for SLS-AC that considers only autocorrelation (Figure 6b).

With respect to parametric uncertainty estimation, Figures 7c and 7d show that sharpness generally increases when the three assumptions in the data models are gradually relaxed from SLS to WSEP-AC. This is even more obvious during the validation period. Given that the prediction ensemble does not center on the data, the increasing sharpness is desirable as it improves reliability. This is confirmed by the reliability plots in Figures 7e and 7f. The exceptions are again for SLS-AC and SEP-AC that generally have the lowest coverage.

With respect to the overall predictive performance measured by RMS, the same variation pattern and exception are also observed in the RMS plots in Figures 7g and 7h. This is not surprising because RMS is the metric that can be used to measure all the three criteria (central mean tendency, sharpness, and reliability). Since the prediction ensemble is not centered on the data, the sharpness and reliability are the decisive factors for evaluating the predictive performance.

As a summary, while it is necessary to account for heteroscedasticity in a data model, caution is needed when accounting for autocorrelation in the manner described in Section 2.1. In addition, after comparing the RMS values of the residuals using the Gaussian and SEP distributions, the conclusion is that the SEP distribution outperforms the Gaussian distribution with respect to predictive performance. Finally, uncertainty underestimation is evidenced by the very small predictive coverage. The underestimation of uncertainty for all the physical models with all the data model is not unexpected because only parametric uncertainty is considered in this study. Considering the overall predictive uncertainty is the subject of the next section.

## 4.2 Predictive performance with total uncertainty

The simulated output $\mathbf{Y}(\boldsymbol{\theta}_p)$ is generally not equal to the observed output $\mathbf{d}$, and we have a residual term $\boldsymbol{\varepsilon}$ due to measurement, input and model structure errors such that $\mathbf{d} = \mathbf{Y}(\boldsymbol{\theta}_p) + \boldsymbol{\varepsilon}$. Accounting for the error term $\boldsymbol{\varepsilon}$ can be through separating various error terms. For example, in section 4.1 we obtained uncertainty due to the physical model parameters. Accounting for other sources of uncertainty can be done using a single model approach (e.g. Thyer et al., 2009) or a multi-model approach (e.g. Tsai and Elshall, 2013). Alternatively, we can quantify the uncertainty based on total residuals that separates out parametric uncertainty, so the residual error includes errors in measurements, model inputs, and model structures (e.g. Thyer et al., 2009; Schoups and Vrugt, 2010). This lumped approach is based on sampling the residuals model $\boldsymbol{\varepsilon}(\boldsymbol{\theta}_{\varepsilon})$ with parameters $\boldsymbol{\theta}_{\varepsilon}$. SLS has one fixed parameter that is the constant variance, and other data models have two to six parameters. Thus in this section the prediction ensemble addresses parametric uncertainty of not only the soil respiration models but also the data models. When generating the prediction ensemble in the procedure described by Schoups and Vrugt (2010), an ensemble of residuals is first generated by running the data models with posterior samples of the data model parameters for the positive carbon efflux domain; the residual ensemble is then added to the prediction ensemble generated in Section 4.1.

We start by a visual assessment of the predictive performance. Figure 8 is similar to Figure 6 with the exception that Figure 8 considers the overall predictive uncertainty (i.e. parametric and output uncertainty), while Figure 6 considers the parametric uncertainty only. Figure 8 reveals a practical observation about accounting for the overall uncertainty through the lumped approach of sampling the data models. For example, Figure 8b shows that, despite the wide prediction interval of model 4C, the model with significant model structure error cannot capture the birch pulse around

640 day 180. It indicates that proper using a data model for model residuals cannot compensate
641 significant model structure error.

642 Figure 9 plots the four statistics (NSME, sharpness, predictive coverage, and RMS) of the three
643 soil respiration models under the eight data models to assess the predictive performance. With
644 respect to central mean tendency, the NSME values in Figures 9a-9b are visually the same as those
645 in Figures 7a-7b, indicating that the central mean accuracy under parametric uncertainty is the
646 same as that under predictive uncertainty.

647 With respect to uncertainty, the values of sharpness and predictive coverage increase
648 substantially (Figures 9c – 9f). In particular, Figures 9e and 9f show that, except for SLS and SEP,
649 the predictive coverage of the rest of the six data models are close to 100% for all the three soil
650 respiration models, indicating that the prediction intervals cover almost all the data. This is
651 demonstrated in Figures 6 for WSEP-AC. Similar to Figures 7c and 7d, Figures 9c and 9d also
652 show a general pattern that the sharpness increases when the three assumptions in the data models
653 are gradually relaxed from SLS to WSEP-AC. The data models that account for autocorrelation
654 are still the exceptions.

655 With respect to the overall predictive performance, the RMS values are largely determined by
656 the mean accuracy and sharpness as the predictive coverage is similar for different data models.
657 Figures 9g and 9h of RMS show that the predictive performance of the four data models that
658 account for autocorrelation is worse than that of the other four data models. This suggests again
659 that one needs to be cautious when building autocorrelation into a data model. This is consistent
660 with the finding of Evin et al. (2013, 2014) that accounting for autocorrelation before accounting
661 for heteroscedasticity or jointly accounting for autocorrelation and heteroscedasticity can result in
662 poor predictive performance. In summary, Figures 9g and 9h show for both the calibration and

prediction periods that accounting for heteroscedasticity in WLS and WSEP gives the best overall predictive performance, and accounting for autocorrelation without heteroscedasticity in SLS-AC and SEP-AC gives the worst overall predictive performance. Finally, for the three soil respiration models, RMS shows that model 4C has the worst predictive performance for both the calibration and cross-validation data. Generally speaking, the high fidelity model 6C outperforms model 5C for both the calibration and cross-validation data, which justifies the complexity of model 6C.

To demonstrate the impacts of the data models on predictive performance of the soil respiration models, Figure 10 plots the model simulations and predictions given by model 6C during the calibration and cross-validation periods using all the eight data models. Figure 10 is used to investigate predictive performance characteristics of the different data models. By examining the predictive performance of model 6C, specific predictive performance patterns can be identified. Figures 10a – 10d show that SLS and SEP have similar predictive performance with SEP generally having better predictive performance especially during the validation period. Not accounting for heteroscedasticity will underestimate the predication uncertainty (Figure 10b and Figure 10d). This is mainly because the variance of the efflux residuals increases with the magnitude of the carbon effluxes (Figure 3a), and thus assuming constant variance is not representative. Accordingly, accounting for heteroscedasticity using WLS (Figure 10e) or WSEP (Figure 10h) will make the predictions more sensitive to peaek carbon effluxes. This will generally improve the predictive coverage on the expense of sharpness and the central mean tendency. While WLS and WSEP have similar predictive performance, WSEP has better central mean tendency and overall predictive performance than WLS. Figures 10i – 10l show that accounting for autocorrelation using SLS-AC and SEP-AC results in wider uncertainty bands and insensitivity to peak carbon effluxes as compared to SLS and SEP (Figures 10a-d), which may be due to reduction of information content

of the residuals. This results in deteriorating the sharpness, the central mean tendency and the capturing of peak carbon fluxes, especially during the validation period. Figures 10m – 10p show that accounting for both heteroscedasticity and autocorrelation using WLS-AC and WSEP-AC makes the inference robust against peak carbon effluxes. However, due to the loss of information content, the uncertainty bands are still wider, and uncertainty becomes overestimated especially during validation period as compared to WLS and WSEP (Figures 10e – 10h). The results of Models 4C and 5C, which are not shown here, also show the same prediction patterns with respect to non-Gaussian residuals, heteroscedasticity, and autocorrelation.

Finally, we observe in Figure 10 that the data models that have good overall predictive performance as measured by RMS during the calibration period will maintain this good predictive performance during the validation period. For model 6C, RMS values for the calibration and validation periods are very well correlated with a correlation coefficient of 0.92. However, we note that for models 4C and 5C the overall predictive performances during the calibration and validation periods are not that well correlated as 6C, with correlation coefficients of 0.52 for model 4C and 0.61 for model 5C. This suggests that model 6C is more robust than 4C and 5C for forecasting and hindcasting.

### 4.3 Discussion on handling residual correlation

Accounting for autocorrelation can lead to biased parameter estimation (Figure 5) and poor predictive performance (Figure 10). Auto-correlated residuals may be attributed to model discrepancy, as shown in Lu et al. (2013). The most obvious solution to handle the autocorrelation is to reduce the autocorrelation by improving the soil respiration model. If model improvement is difficult for practical reasons, we can improve the data model to better characterize the

708 autocorrelation. Addressing autocorrelation in a data model is challenging since it involves several
709 interlinked factors as follows:
710 (1) Non-stationarity due to wet-dry periods could be a reason for this problem. By drawing on
711 similarity from surface hydrology, the study of Ammann et al. (2018) suggests that auto-
712 correlated residuals might be attributed to non-stationarity due to wet-dry periods with half-
713 hourly data. Accounting for non-stationarity could better address the problem of auto-
714 correlated residuals (Ammann et al., 2018; Smith et al., 2010b).
715 (2) The way of implementing autocorrelation could have an impact. Autocorrelation could be
716 applied to raw residuals directly (e.g., Li et al., 2015), to transformed residuals based on
717 covariance matrix of residuals L(**e**) (e.g., Lu et al., 2013), or to normalized residuals L(**a**) (e.g.,
718 Schoups and Vrugt, 2010; Evin et al., 2013). Note that **e** is a vector of transformed residuals,
719 while **a** denotes a vector of independent and identically distributed random errors with zero
720 mean and unit standard deviation. The L(**e**) approach based on covariance matrix of residuals
721 is generally limited to Gaussian data models (e.g. Lu et al., 2013), while the L(**a**) approach for
722 normalized residuals can be readily adopted for non-Gaussian data models.
723 (3) The autocorrelation model could have an impact. Using an autoregressive model is a popular
724 technique to account for auto-correlated residuals. However, using an autoregressive model
725 with either joint inversion approach (e.g., this study and Schoups and Vrugt, 2010) or
726 sequential approaches (e.g., Evin et al., 2013, 2014; Lu et al., 2013) removes correlation errors
727 through a filter approach, which can lead to a loss of information content. As this may cause
728 overcorrection of prediction especially at surge events, Li et al. (2015) developed a restricted
729 autoregressive model to overcome this adverse effect. Other autocorrelation models include
730 moving average model and mixed autoregressive-moving averaging model (Chatfield, 2004).

(4) Joint versus sequential inversion for autocorrelation could have an impact. Sequential inversion approaches include two-step procedures (e.g. Evin et al., 2013, 2014; Lu et al., 2013) or the multi-step procedure (Li et al., 2016a). These sequential approach estimates the autoregressive parameters sequentially in a later step after estimating the physical model parameters and other data model parameters. Evin et al. (2013, 2014) used a sequential approach to avoid the interaction between the parameters of the heteroscedasticity model and the autocorrelation model. In addition, the autoregressive model parameters can be deterministically calculated as an internal variables of the data model similar to Lu et al. (2013), and not as calibration parameters (e.g. Schoups and Vrugt; Evin et al. 2013; 2014). While the first step in the sequential approach would avoid the biased parameter estimation (Figure 10a-d), the second step can still lead a poor predicative performance since we are essentially using a filter approach to remove residual correlation. To address this problem, Li et al. (2016) multi-step procedure that is based on Gaussian data model uses restricted autoregressive model. Generally, Ammann et al. (2018) states that the joint inversion is still preferred, and understanding the conditions where accounting for auto-correlation can be achieved remains poorly understood.

## 5. Conclusions

In parameter estimation and prediction of soil carbon fluxes to the atmosphere, one often assumes that residuals, which include errors in observations, model inputs, parameter estimates, and model structures, are normally distributed, homoscedastic and uncorrelated. We study these assumptions by calibrating three soil ~~inspiration~~ respiration models, which have varying degrees of model structure errors. We further explore eight data models that characterize the residuals statistically by starting with the standard least squares (SLS) and skew exponential power (SEP)

754 data models that assume homoscedastic and non-correlated residuals. For these two distributions,
755 we evaluate six other data models that account for heteroscedasticity (WLS and WSEP),
756 autocorrelation (SLS-AC and SEP-AC), and joint inversion of heteroscedasticity and
757 autocorrelation (WLS-AC and WSEP-AC). To our knowledge this is the first study that provides
758 such detailed analysis for soil reparation inverse modeling. We also use three soil respiration
759 models with different degrees of model fidelity (i.e., model discrepancy) and model complexity
760 (i.e. number of model parameters) to understand the impact of model discrepancy on the calibration
761 results under different data models. We analyze the results with respect to (1) residual
762 characterization, (2) parameter estimation, (3) predictive performance, and (4) impacts of model
763 discrepancy. The main findings of this study are summarized as follows:

764 (1) With respect to residual characterization, residual analysis results suggest that the common
765 assumption of not accounting for heteroscedasticity and residual autocorrelation in the data
766 models SLS and SEP results in poor characterization of residuals. Explicit accounting for
767 heteroscedasticity in WLS and WSEP results in significantly improved characterization of the
768 residuals, and the improvement is larger than that obtained by accounting for both
769 heteroscedasticity and autocorrelation in WSL-AC and WSEP-AC. Accounting for
770 autocorrelation only in SLS-AC and SEP-AC does not significantly improve the
771 characterization of the residuals.

772 (2) With respect to parameter estimation, the impacts of the data models are evaluated by focusing
773 on carbon use efficiency (CUE), which is a central parameter in soil respiration modeling.
774 Using SLS yields relatively reasonable posterior parameter distributions for CUE , yet very
775 narrow posterior. The data models SLS-AC, SEP-AC, WLS-AC and WSEP-AC that consider
776 autocorrelation tend to yield CUE estimates that are physically unreasonable. We speculate

777 that filtering residual correlation can affect the mapping of the model physics (as implicitly
778 included in the residuals) into the parameter space, which might result in biased parameter
779 estimates that are physically unreasonable.
780 (3) With respect to predictive performance, it is measured by four statistical criteria: central mean
781 tendency, sharpness, coverage, and relative model score for both the calibration and the cross-
782 validation periods. Results show that accounting for autocorrelation in SLS-AC, SEP-AC,
783 WLS-AC, and WSEP-AC deteriorates the predicative performance, such that the predictive
784 performance is inferior to that of SLS in terms of the central mean tendency and overall
785 predictive performance (measured by the relative model score), especially during the cross-
786 validation period. Results also indicates that using the SEP distribution can potentially improve
787 the predictive performance. The same is true for accounting for heteroscedasticity. Using SEP
788 distribution and accounting for heteroscedasticity (i.e. WSEP) can potentially improve the
789 predictive performance.
790 (4) With respect to the impact of model discrepancy, the high fidelity model (6C) gives the best
791 results with respect to parameter estimation and predictive performance. Model 6C generally
792 maintains its superior performance under different data models. This justifies the complexity
793 of model 6C relative to model 5C that has one less carbon pool. Model 4C with the lowest
794 fidelity maintains its poor performance for different data models, because the model has only
795 four carbon pools and lacks the explicit representation of soil moisture control.
796 Based on the empirical findings above, we conclude the following:
797 (1) Not accounting for heteroscedasticity and autocorrelation using a Gaussian or non-Gaussian
798 data model might not necessarily result in biased parameter estimates or biased predictions

with respect to central mean tendency, but will definitely underestimate uncertainty resulting in lower overall predictive performance.

(2) Using a non-Gaussian data model can improve parameter estimation and predictive performance with respect to central mean tendency and uncertainty quantification.

(3) Accounting for heteroscedasticity improves the uncertainty estimation with respect to reliability at the cost of having a wider predictive interval.

(4) This study confirms other empirical findings and theoretical analyses (Evin et al., 2013; 2014; Li et al., 2015, Ammann et al. 2018) that separately accounting for autocorrelation or jointly accounting for autocorrelation and heteroscedasticity can be problematic. While the reasons remain poorly understood (Ammann et al., 2018), it might be attributed to non-stationarity due to wet-dry periods with half-hourly data (Ammann et al., 2018) or to the method of handling autocorrelation (e.g., Schoups and Vrugt, 2010, Evin et al., 2013; 2014; Lu et al., 2013; Li et al., 2015, 2016a; Ammann et al. 2018). Further investigation to address autocorrelation in soil respiration modeling is warranted in a future study.

The above conclusions are subject to several limitations. First, the conclusions are specific to the soil respiration models developed and validated for semi-arid savannah. Performance variations across different soil respiration models with different levels of complexities is possible. Second, the conclusions are conditioned on the data that were obtained at the half-hour interval over a one-year period. Different conclusions are possible if the data are thinned to daily or weekly scales or data of longer observation periods are used. Third, our study investigates effects of the residual assumptions of formal likelihood functions through direct conditioning of the residuals model parameters, yet this can also be done through other approaches such as residuals transformation (Thiemann et al., 2001), autorgressive bias model (Del Giudice et al., 2013),

822 approximate Bayesian computation (Sadegh and Vrugt, 2013), and data assimliation (Spaaks and
823 Bouten, 2013). Comparing different methods for accounting the residual assumptions are beyond
824 the scope of this work. Fourth, this study focuses on formal Bayesian computation using formal
825 likelihood functions, and comparison with other inference functions such as informal likelihood
826 functions or approximate Bayesian computation is warranted in a future study.

827 Based on the aforesaid conclusions and limitations, we recommend to start calibrating soil
828 respiration models with simple SLS or SEP likelihood function. If the residuals characterization is
829 adequate (e.g., Scharnagl et al., 2011), then the underlying assumptions are met. Otherwise,
830 increase complexity of the data model until satisfactory results are obtained in terms of residuals
831 characterization, posterior parameter estimation, and predictive performance. This is similar to the
832 procedure given in Smith et al. (2015). Although the empirical findings of this study provide
833 general guidelines for data model selection for soil respiration modeling, more comparative studies
834 are needed to validate and refute the findings of this study.

835 **Acronyms**

| | |
|---|---|
| 836 4C | Four carbon pool model |
| 837 5C | Five carbon pool model |
| 838 6C | Six carbon pool model |
| 839 CUE | Microbial carbon use efficiency |
| 840 DOC | Dissolved organic carbon |
| 841 ENZ | Enzymes |
| 842 MCMC | Markov chain Monte Carlo |
| 843 MIC | Microbial biomass |
| 844 NSME | Nash-Sutcliffe model efficiency |
| 845 PDF | Probability density function |
| 846 RMS | Relative model score |
| 847 SEP | Skew exponential power distribution |
| 848 SEP-AC | Skew exponential power distribution with autocorrelation |
| 849 SLS | Standard least square |
| 850 SLS-AC | Standard least square with autocorrelation |
| 851 SOC | Soil organic carbon |
| 852 WLS | Weighted least squared |
| 853 WLS-AC | Weight least square with autocorrelation |

WSEP Weighted skew exponential power distribution
WSEP-AC Weighted skew exponential power distribution with autocorrelation

## Code and data availability

The data and codes and models used to produce this paper are available on contact of the corresponding author at mye@fsu.edu. We cannot publicly share the workflow because MT-DREAM$_{(ZS)}$ code (Laloy and Vrugt, 2012) , which is a main component in the workflow, is in the process of becoming a commercial code.

## Author contributions

ASE developed and implemented the code for the eight data models for soil respiration modeling, and prepared the manuscript with contribution of all co-authors. MY developed the research idea and outline, and supervised the research implementation when ASE was a post-doc at Florida State University. GN developed the soil respiration models. GAB collected and processed the eddy-covariance data used for model calibration.

## Competing interests

The authors declare that they have no conflict of interest.

## Acknowledgement

The first two authors were supported by the U.S. Department of Energy grant DE-SC0008272. The first author was also partly supported by the U.S. National Science Foundation Award# OIA-1557349. The second author was also partly supported by U.S. Department of Energy grant DE-SC0019438 and U.S. National Science Foundation grant EAR-1552329. We thank two anonymous reviewers for providing comments that helped to improve the manuscript.

## References

Ahrens, B., Reichstein, M., Borken, W., Muhr, J., Trumbore, S. E. and Wutzler, T.: Bayesian calibration of a soil organic carbon model using ΔC measurements of soil organic carbon

879 and heterotrophic respiration as joint constraints, Biogeosciences, 11(8), 2147–2168,
880 doi:10.5194/bg-11-2147-2014, 2014.
881 Allison, S. D., Wallenstein, M. D. and Bradford, M. A.: Soil-carbon response to warming
882 dependent on microbial physiology, Nat. Geosci., 3, 336 [online] Available from:
883 http://dx.doi.org/10.1038/ngeo846, 2010.
884 Ammann, L., Reichert, P. and Fenicia, F.: A framework for likelihood functions of deterministic
885 hydrological models, Hydrol. Earth Syst. Sci., (August), 2018.
886 Bagnara, M., Sottocornola, M., Cescatti, A., Minerbi, S., Montagnani, L., Gianelle, D. and
887 Magnani, F.: Bayesian optimization of a light use ef fi ciency model for the estimation of
888 daily gross primary productivity in a range of Italian forest ecosystems, Ecol. Modell., 306,
889 57–66, doi:10.1016/j.ecolmodel.2014.09.021, 2015.
890 Bagnara, M., Oijen, M. Van, Cameron, D., Gianelle, D., Magnani, F. and Sottocornola, M.:
891 Bayesian calibration of simple forest models with multiplicative mathematical structure :
892 A case study with two Light Use E ffi ciency models in an alpine forest, Ecol. Modell.,
893 371(January), 90–100, doi:10.1016/j.ecolmodel.2018.01.014, 2018.
894 Barr, J. G., Engel, V., Fuentes, J. D., Fuller, D. O. and Kwon, H.: Modeling light use efficiency in
895 a subtropical mangrove forest equipped with CO2eddy covariance, Biogeosciences, 10(3),
896 2145–2158, doi:10.5194/bg-10-2145-2013, 2013.
897 Barron-gafford, G. A., Cable, J. M., Bentley, L. P., Scott, R. L., Huxman, T. E., Jenerette, G. D.
898 and Ogle, K.: Quantifying the timescales over which exogenous and endogenous
899 conditions affect soil respiration, New Phytol., 2014.
900 Barron-Gafford, G. A., Scott, R. L., Jenerette, G. D. and Huxman, T. E.: The relative controls of
901 temperature, soil moisture, and plant functional group on soil CO<inf>2</inf> efflux at

902 diel, seasonal, and annual scales, J. Geophys. Res. Biogeosciences, 116(1), 1–16,
903 doi:10.1029/2010JG001442, 2011.
904 Berryman, E. M., Frank, J. M., Massman, W. J. and Ryan, M. G.: Agricultural and Forest
905 Meteorology Using a Bayesian framework to account for advection in seven years of
906 snowpack CO 2 fl uxes in a mortality-impacted subalpine forest, Agric. For. Meteorol.,
907 249(April 2017), 420–433, doi:10.1016/j.agrformet.2017.11.004, 2018.
908 Box, G. E. P. and Tiao, G. C.: Bayesian inference in statistical analysis, Wiley., 1992.
909 Braakhekke, M. C., Beer, C., Schrumpf, M., Ekici, A., Ahrens, B., Hoosbeek, M. R., Kruijt, B.,
910 Kabat, P. and Reichstein, M.: The use of radiocarbon to constrain current and future soil
911 organic matter turnover and transport in a temperate forest, J. Geophys. Res.
912 Biogeosciences, 372–391, doi:10.1002/2013JG002420.Received, 2014.
913 Bradford, M. A., Davies, C. A., Frey, S. D., Maddox, T. R., Melillo, J. M., Mohan, J. E., Reynolds,
914 J. F., Treseder, K. K. and Wallenstein, M. D.: Thermal adaptation of soil microbial
915 respiration to elevated temperature, Ecol. Lett., 11(12), 1316–1327, doi:10.1111/j.1461-
916 0248.2008.01251.x, 2008.
917 Braswell, B. H., Sacks, W. J., Linder, E. and Schimel, D. S.: Estimating diurnal to annual
918 ecosystem parameters by synthesis of a carbon flux model with eddy covariance net
919 ecosystem exchange observations, Glob. Chang. Biol., 335–355, doi:10.1111/j.1365-
920 2486.2005.00897.x, 2015.
921 Cable, J. M., Ogle, K., Williams, D. G., Weltzin, J. F. and Huxman, T. E.: Soil Texture Drives
922 Responses of Soil Respiration to Precipitation Pulses in the Sonoran Desert : Implications
923 for Climate Change, Ecosystems, 961–979, doi:10.1007/s10021-008-9172-x, 2008.
924 Cable, J. M., Ogle, K., Lucas, R. W., Huxman, T. E., Loik, M. E., Smith, S. D., Tissue, D. T.,

925 Ewers, B. E., Pendall, E., Welker, J. M., Charlet, T. N., Cleary, M., Griffith, A., Nowak,
926 R. S., Rogers, M., Steltzer, H., Sullivan, P. F. and Gestel, N. C. Van: The temperature
927 responses of soil respiration in deserts : a seven desert synthesis, Biogeochemistry, 71–90,
928 doi:10.1007/s10533-010-9448-z, 2011.
929 Chatfield, C.: The analysis of time series : an introduction, Chapman & Hall/CRC. [online]
930 Available from: https://www.crcpress.com/The-Analysis-of-Time-Series-An-
931 Introduction-Sixth-Edition/Chatfield/p/book/9781584883173 (Accessed 9 April 2019),
932 2004.
933 Chevallier, F. and O'Dell, C. W.: Error statistics of Bayesian CO2flux inversion schemes as seen
934 from GOSAT, Geophys. Res. Lett., 40(6), 1252–1256, doi:10.1002/grl.50228, 2013.
935 Correia, A. C., Minunno, F., Caldeira, M. C., Banza, J., Mateus, J., Carneiro, M., Wingate, L.,
936 Shvaleva, A., Ramos, A., Jongen, M., Bugalho, M. N., Nogueira, C., Lecomte, X. and
937 Pereira, J. S.: Agriculture , Ecosystems and Environment Soil water availability strongly
938 modulates soil CO 2 efflux in different Mediterranean ecosystems : Model calibration
939 using the Bayesian approach, Agric. Ecosyst. Environ., 161, 88–100,
940 doi:10.1016/j.agee.2012.07.025, 2012.
941 Davidson, E. A. and Janssens, I. A.: Temperature sensitivity of soil carbon decomposition and
942 feedbacks to climate change, Nature, 440, 165 [online] Available from:
943 http://dx.doi.org/10.1038/nature04514, 2006.
944 Davidson, E. A., Samanta, S., Caramori, S. S. and Savage, K.: The Dual Arrhenius and Michaelis–
945 Menten kinetics model for decomposition of soil organic matter at hourly to seasonal time
946 scales, Glob. Chang. Biol., 18(1), 371–384, doi:10.1111/j.1365-2486.2011.02546.x, 2011.
947 Du, Z., Nie, Y., He, Y., Yu, G. and Wang, H.: Tellus B : Chemical and Physical Meteorology

948 Complementarity of flux- and biometric-based data to constrain parameters in a terrestrial
949 carbon model Complementarity of flux- and biometric-based data to constrain parameters
950 in a terrestrial carbon model, Tellus B Chem. Phys. Meteorol., 0889,
951 doi:10.3402/tellusb.v67.24102, 2015.
952 Du, Z., Zhou, X., Shao, J., Yu, G., Wang, H., Zhai, D., Xai, J. and Luo, Y.: Journal of Advances
953 in Modeling Earth Systems, J. Adv. Model. Earth Syst., 548–565,
954 doi:10.1002/2016MS000687.Received, 2017.
955 Elshall, A. S. and Tsai, F. T.-C.: Constructive epistemic modeling of groundwater flow with
956 geological structure and boundary condition uncertainty under the Bayesian paradigm, J.
957 Hydrol., 517, doi:10.1016/j.jhydrol.2014.05.027, 2014.
958 Elshall, A. S., Ye, M., Pei, Y., Zhang, F., Niu, G.-Y. and Barron-Gafford, G. A.: Relative model
959 score: a scoring rule for evaluating ensemble simulations with application to microbial soil
960 respiration modeling, Stoch. Environ. Res. Risk Assess., doi:10.1007/s00477-018-1592-3,
961 2018a.
962 Elshall, A. S., Ye, M., Pei, Y., Zhang, F., Niu, G.-Y. and Barron-Gafford, G. A.: Relative model
963 score: a scoring rule for evaluating ensemble simulations with application to microbial soil
964 respiration modeling, Stoch. Environ. Res. Risk Assess., 32(10), 2809–2819,
965 doi:10.1007/s00477-018-1592-3, 2018b.
966 Evin, G., Kavetski, D., Thyer, M. and Kuczera, G.: Pitfalls and improvements in the joint inference
967 of heteroscedasticity and autocorrelation in hydrological model calibration, Water Resour.
968 Res., 49(7), 4518–4524, doi:10.1002/wrcr.20284, 2013.
969 Evin, G., Thyer, M., Kavetski, D., McInerney, D. and Kuczera, G.: Comparison of joint versus
970 postprocessor approaches for hydrological uncertainty estimation accounting for error

971 autocorrelation and heteroscedasticity, Water Resour. Res., 50(3), 2350–2375,
972 doi:10.1002/2013WR014185, 2014.
973 Fernández-Martínez, M., Vicca, S., Janssens, I. A., Sardans, J., Luyssaert, S., Campioli, M.,
974 Chapin III, F. S., Ciais, P., Malhi, Y., Obersteiner, M., Papale, D., Piao, S. L., Reichstein,
975 M., Rodà, F. and Peñuelas, J.: Nutrient availability as the key regulator of global forest
976 carbon balance, Nat. Clim. Chang., 4, 471 [online] Available from:
977 http://dx.doi.org/10.1038/nclimate2177, 2014.
978 Gelman, A. and Rubin, D. B.: Inference from Iterative Simulation Using Multiple Sequences, Stat.
979 Sci., 7(4), 457–472, doi:10.1214/ss/1177011136, 1992.
980 German, D. P., Marcelo, K. R. B., Stone, M. M. and Allison, S. D.: The Michaelis–Menten kinetics
981 of soil extracellular enzymes in response to temperature: a cross-latitudinal study, Glob.
982 Chang. Biol., 18(4), 1468–1479, doi:10.1111/j.1365-2486.2011.02615.x, 2011.
983 Del Giudice, D., Honti, M., Scheidegger, A., Albert, C., Reichert, P. and Rieckermann, J.:
984 Improving uncertainty estimation in urban hydrological modeling by statistically
985 describing bias, Hydrol. Earth Syst. Sci., 17(10), 4209–4225, doi:10.5194/hess-17-4209-
986 2013, 2013.
987 Gragne, A. S., Sharma, A., Mehrotra, R. and Alfredsen, K.: Improving real-time inflow forecasting
988 into hydropower reservoirs through a complementary modelling framework, Hydrol. Earth
989 Syst. Sci., 19(8), 3695–3714, doi:10.5194/hess-19-3695-2015, 2015.
990 Hararuk, O., Xia, J. and Luo, Y.: Evaluation and improvement of a global land model against soil
991 carbon data using a Bayesian Markov chain Monte Carlo method, J. Geophys. Res.
992 Biogeosciences, 119(3), 403–417, doi:10.1002/2013JG002535, 2014.
993 Hashimoto, S., Morishita, T., Sakata, T., Ishizuka, S., Kaneko, S. and Takahashi, M.: Simple

994 models for soil CO2, CH4, and N2O fluxes calibrated using a Bayesian approach and
995 multi-site data, Ecol. Modell., 222(7), 1283–1292, doi:10.1016/j.ecolmodel.2011.01.013,
996 2011.
997 He, H., Meyer, A., Jansson, P., Svensson, M., Rütting, T. and Klemedtsson, L.: Simulating
998 ectomycorrhiza in boreal forests : implementing ectomycorrhizal fungi model MYCOFON
999 in CoupModel ( v5 ), Geosci. Model Dev., 725–751, 2018.
1000 Hilton, T. W., Davis, K. J. and Keller, K.: Evaluating terrestrial CO2flux diagnoses and
1001 uncertainties from a simple land surface model and its residuals, Biogeosciences, 11(2),
1002 217–235, doi:10.5194/bg-11-217-2014, 2014.
1003 Hoeting, J. A., Madigan, D., Raftery, A. E. and Volinsky, C. T.: Bayesian model averaging: a
1004 tutorial (with comments by M. Clyde, David Draper and E. I. George, and a rejoinder by
1005 the authors, Stat. Sci., 14(4), 382–417, doi:10.1214/ss/1009212519, 1999.
1006 Högberg, P. and Read, D. J.: Towards a more plant physiological perspective on soil ecology,
1007 Trends Ecol. Evol., 21(10), 548–554, doi:10.1016/j.tree.2006.06.004, 2006.
1008 Hublart, P., Ruelland, D., De Cortázar-Atauri, I. G., Gascoin, S., Lhermitte, S. and Ibacache, A.:
1009 Reliability of lumped hydrological modeling in a semi-arid mountainous catchment facing
1010 water-use changes, Hydrol. Earth Syst. Sci., 20(9), 3691–3717, doi:10.5194/hess-20-3691-
1011 2016, 2016.
1012 Ishikura, K., Yamada, H., Toma, Y., Takakai, F., Darung, U., Limin, A. and Limin, S. H.: Soil
1013 Science and Plant Nutrition Effect of groundwater level fluctuation on soil respiration rate
1014 of tropical peatland in Central Kalimantan , Indonesia, Soil Sci. Plant Nutr., 63(1), 1–13,
1015 doi:10.1080/00380768.2016.1244652, 2017.
1016 Janssens, I. A., Freibauer, A., Ciais, P., Smith, P., Nabuurs, G.-J., Folberth, G., Schlamadinger, B.,

1017 Hutjes, R. W. A., Ceulemans, R., Schulze, E.-D., Valentini, R. and Dolman, A. J.: Europe's
1018 terrestrial biosphere absorbs 7 to 12% of European anthropogenic CO2 emissions.,
1019 Science, 300(5625), 1538–42, doi:10.1126/science.1083592, 2003.
1020 Katz, R. W., Craigmile, P. F., Guttorp, P., Haran, M., Sansó, B. and Stein, M. L.: Uncertainty
1021 analysis in climate change assessments, Nat. Clim. Chang., 3, 769 [online] Available from:
1022 http://dx.doi.org/10.1038/nclimate1980, 2013.
1023 Kavetski, D., Franks, S. W. and Kuczera, G.: Confronting Input Uncertainty in Environmental
1024 Modelling, Calibration Watershed Model., doi:doi:10.1029/WS006p0049, 2013.
1025 Keenan, T. F., Davidson, E., Moffat, A. M., Munger, W. and Richardson, A. D.: Using model-data
1026 fusion to interpret past trends, and quantify uncertainties in future projections, of terrestrial
1027 ecosystem carbon cycling, Glob. Chang. Biol., 18(8), 2555–2569, doi:10.1111/j.1365-
1028 2486.2012.02684.x, 2012.
1029 Kim, Y., Nishina, K., Chae, N., Park, S. J., Yoon, Y. J. and Lee, B. Y.: Constraint of soil moisture
1030 on CO 2 efflux from tundra lichen , moss , and tussock in Council , Alaska , using a
1031 hierarchical Bayesian model, Biogeosciences, 5567–5579, doi:10.5194/bg-11-5567-2014,
1032 2014.
1033 Klemedtsson, L., Jansson, P. E., Gustafsson, D., Karlberg, L., Weslien, P., Von Arnold, K.,
1034 Ernfors, M., Langvall, O. and Lindroth, A.: Bayesian calibration method used to elucidate
1035 carbon turnover in forest on drained organic soil, Biogeochemistry, 89(1), 61–79,
1036 doi:10.1007/s10533-007-9169-0, 2008.
1037 Laloy, E. and Vrugt, J. A.: High-dimensional posterior exploration of hydrologic models using
1038 multiple-try DREAM(ZS) and high-performance computing, Water Resour. Res., 48(1),
1039 doi:10.1029/2011WR010608, 2012.

Li, J., Wang, G., Allison, S. D., Mayes, M. A. and Luo, Y.: Soil carbon sensitivity to temperature and carbon use efficiency compared across microbial-ecosystem models of varying complexity, Biogeochemistry, 119, 67–84 [online] Available from: http://www.jstor.org/stable/24716883, 2014.

Li, M., Wang, Q. J., Bennett, J. C. and Robertson, D. E.: A strategy to overcome adverse effects of autoregressive updating of streamflow forecasts, Hydrol. Earth Syst. Sci., 19(1), 1–15, doi:10.5194/hess-19-1-2015, 2015.

Li, M., Wang, Q. J., Bennett, J. C. and Robertson, D. E.: Error reduction and representation in stages (ERRIS) in hydrological modelling for ensemble streamflow forecasting, Hydrol. Earth Syst. Sci., 20(9), 3561–3579, doi:10.5194/hess-20-3561-2016, 2016a.

Li, Q., Xia, J., Shi, Z., Huang, K., Du, Z. and Lin, G.: Variation of parameters in a Flux-Based Ecosystem Model across 12 sites of terrestrial ecosystems in the conterminous USA, Ecol. Modell., 336, 57–69, doi:10.1016/j.ecolmodel.2016.05.016, 2016b.

Lu, D., Ye, M., Meyer, P. D., Curtis, G. P., Shi, X., Niu, X.-F. and Yabusaki, S. B.: Effects of error covariance structure on estimation of model averaging weights and predictive performance, Water Resour. Res., 49(9), 6029–6047, doi:10.1002/wrcr.20441, 2013.

Luo, Y., Ogle, K., Tucker, C., Fei, S., Gao, C., LaDeau, S., Clark, J. S. and Schimel, D. S.: Ecological forecasting and data assimilation in a data-rich era, Ecol. Appl., 21(5), 1429–1442, doi:10.1890/09-1275.1, 2011.

Luo, Y., Keenan, T. F. and Smith, M.: Predictability of the terrestrial carbon cycle, Glob. Chang. Biol., 21(5), 1737–1751, doi:10.1111/gcb.12766, 2014.

Manzoni, S., Taylor, P., Richter, A., Porporato, A. and Ågren, G. I.: Environmental and stoichiometric controls on microbial carbon-use efficiency in soils, New Phytol., 196(1),

79–91, doi:10.1111/j.1469-8137.2012.04225.x, 2012.

McInerney, D., Thyer, M., Kavetski, D., Lerat, J. and Kuczera, G.: Improving probabilistic prediction of daily streamflow by identifying Pareto optimal approaches for modeling heteroscedastic residual errors, Water Resour. Res., 53, 2199–2239, doi:10.1002/2016WR019168.Received, 2017.

Menichetti, L., Kätterer, T. and Leifeld, J.: Parametrization consequences of constraining soil organic matter models by total carbon and radiocarbon using long-term field data, Biogeosciences, 3003–3019, doi:10.5194/bg-13-3003-2016, 2016.

Nash, J. E. and Sutcliffe, J. V: River flow forecasting through conceptual models part I — A discussion of principles, J. Hydrol., 10(3), 282–290, doi:https://doi.org/10.1016/0022-1694(70)90255-6, 1970.

Ogle, K., Ryan, E., Dijkstra, F. A. and Pendall, E.: Journal of Geophysical Research: Biogeosciences, J. Geophys. Res. Biogeoscoences, 1–14, doi:10.1002/2016JG003385, 2016.

Pappenberger, F. and Beven, K. J.: Ignorance is bliss: Or seven reasons not to use uncertainty analysis, Water Resour. Res., 42(5), doi:10.1029/2005WR004820, 2006.

Peters, W., Jacobson, A. R., Sweeney, C., Andrews, A. E., Conway, T. J., Masarie, K., Miller, J. B., Bruhwiler, L. M. P., Pétron, G., Hirsch, A. I., Worthy, D. E. J., van der Werf, G. R., Randerson, J. T., Wennberg, P. O., Krol, M. C. and Tans, P. P.: An atmospheric perspective on North American carbon dioxide exchange: CarbonTracker., Proc. Natl. Acad. Sci. U. S. A., 104(48), 18925–30, doi:10.1073/pnas.0708986104, 2007.

Le Quéré, C., Peters, G. P., Andres, R. J., Andrew, R. M., Boden, T. A., Ciais, P., Friedlingstein, P., Houghton, R. A., Marland, G., Moriarty, R., Sitch, S., Tans, P., Arneth, A., Arvanitis,

A., Bakker, D. C. E., Bopp, L., Canadell, J. G., Chini, L. P., Doney, S. C., Harper, A., Harris, I., House, J. I., Jain, A. K., Jones, S. D., Kato, E., Keeling, R. F., Klein Goldewijk, K., Körtzinger, A., Koven, C., Lefèvre, N., Maignan, F., Omar, A., Ono, T., Park, G.-H., Pfeil, B., Poulter, B., Raupach, M. R., Regnier, P., Rödenbeck, C., Saito, S., Schwinger, J., Segschneider, J., Stocker, B. D., Takahashi, T., Tilbrook, B., van Heuven, S., Viovy, N., Wanninkhof, R., Wiltshire, A. and Zaehle, S.: Global carbon budget 2013, Earth Syst. Sci. Data, 6(1), 235–263, doi:10.5194/essd-6-235-2014, 2014.

Raich, J. W. J. J. W., Potter, C. S. C. and Bhagawati, D.: Interannual variability in global soil respiration, 1980-94, Glob. Chang. Biol., 8, 800–812, doi:10.1046/j.1365-2486.2002.00511.x, 2002.

Ren, X., He, H., Moore, D. J. P., Zhang, L., Liu, M., Li, F., Yu, G. and Wang, H.: Uncertainty analysis of modeled carbon and water fluxes in a subtropical coniferous plantation, J. Geophys. Res. Biogeosciences, 118(4), 1674–1688, doi:10.1002/2013JG002402, 2013.

Ricciuto, D. M., King, A. W., Dragoni, D. and Post, W. M.: Parameter and prediction uncertainty in an optimized terrestrial carbon cycle model: Effects of constraining variables and data record length, J. Geophys. Res. Biogeosciences, 116(1), 1–17, doi:10.1029/2010JG001400, 2011.

Richardson, A. D. and Hollinger, D. Y.: Statistical modeling of ecosystem respiration using eddy covariance data: Maximum likelihood parameter estimation, and Monte Carlo simulation of model and parameter uncertainty, applied to three simple models, Agric. For. Meteorol., 131(3–4), 191–208, doi:10.1016/j.agrformet.2005.05.008, 2005.

Sadegh, M. and Vrugt, J. A.: Bridging the gap between GLUE and formal statistical approaches: Approximate Bayesian computation, Hydrol. Earth Syst. Sci., 17(12), 4831–4850,

1109 doi:10.5194/hess-17-4831-2013, 2013.
1110 Scharnagl, B., Vrugt, J. A., Vereecken, H. and Herbst, M.: Inverse modelling of in situ soil water
1111 dynamics: Investigating the effect of different prior distributions of the soil hydraulic
1112 parameters, Hydrol. Earth Syst. Sci., 15(10), 3043–3059, doi:10.5194/hess-15-3043-2011,
1113 2011.
1114 Schimel, J. P. and Weintraub, M. N.: The implications of exoenzyme activity on microbial carbon
1115 and nitrogen limitation in soil: a theoretical model, Soil Biol. Biochem., 35(4), 549–563,
1116 doi:10.1016/S0038-0717(03)00015-4, 2003.
1117 Schmidt, M. W. I., Torn, M. S., Abiven, S., Dittmar, T., Guggenberger, G., Janssens, I. A., Kleber,
1118 M., Kögel-Knabner, I., Lehmann, J., Manning, D. A. C., Nannipieri, P., Rasse, D. P.,
1119 Weiner, S. and Trumbore, S. E.: Persistence of soil organic matter as an ecosystem
1120 property, Nature, 478(7367), 49–56, doi:10.1038/nature10386, 2011.
1121 Scholz, K., Hammerle, A., Hiltbrunner, E. and Wohlfahrt, G.: Analyzing the Effects of Growing
1122 Season Length on the Net Ecosystem Production of an Alpine Grassland Using Model –
1123 Data Fusion, Ecosystems, 21(5), 982–999, doi:10.1007/s10021-017-0201-5, 2018.
1124 Schoups, G. and Vrugt, J. A.: A formal likelihood function for parameter and predictive inference
1125 of hydrologic models with correlated, heteroscedastic, and non-Gaussian errors, Water
1126 Resour. Res., 46(10), 1–17, doi:10.1029/2009WR008933, 2010.
1127 Scott, R. L., Jenerette, G. D., Potts, D. L. and Huxman, T. E.: Effects of seasonal drought on net
1128 carbon dioxide exchange from a woody-plant-encroached semiarid grassland, J. Geophys.
1129 Res. Biogeosciences, 114(4), doi:10.1029/2008JG000900, 2009.
1130 Shi, X., Ye, M., Curtis, G. P., Miller, G. L., Meyer, P. D., Kohler, M., Yabusaki, S. and Wu, J.:
1131 Assessment of parametric uncertainty for groundwater reactive transport modeling, Water

Resour. Res., 50(5), 4416–4439, doi:10.1002/2013WR013755, 2014.

Sinsabaugh, R. L., Manzoni, S., Moorhead, D. L. and Richter, A.: Carbon use efficiency of microbial communities: stoichiometry, methodology and modelling, Ecol. Lett., 16(7), 930–939, doi:10.1111/ele.12113, 2013.

Smith, M. W., Bracken, L. J. and Cox, N. J.: Toward a dynamic representation of hydrological connectivity at the hillslope scale in semiarid areas, Water Resour. Res., 46(12), doi:10.1029/2009WR008496, 2010a.

Smith, T., Sharma, A., Marshall, L., Mehrotra, R. and Sisson, S.: Development of a formal likelihood function for improved Bayesian inference of ephemeral catchments, Water Resour. Res., 46(12), 1–11, doi:10.1029/2010WR009514, 2010b.

Smith, T., Marshall, L. and Sharma, A.: Modeling residual hydrologic errors with Bayesian inference, J. Hydrol., 528, 29–37, doi:10.1016/j.jhydrol.2015.05.051, 2015.

Spaaks, J. H. and Bouten, W.: Resolving structural errors in a spatially distributed hydrologic model using ensemble Kalman filter state updates, Hydrol. Earth Syst. Sci., 17(9), 3455–3472, doi:10.5194/hess-17-3455-2013, 2013.

Steinacher, M. and Joos, F.: Transient Earth system responses to cumulative carbon dioxide emissions: Linearities, uncertainties, and probabilities in an observation-constrained model ensemble, Biogeosciences, 13(4), 1071–1103, doi:10.5194/bg-13-1071-2016, 2016.

Tang, J. and Riley, W. J.: Weaker soil carbon–climate feedbacks resulting from microbial and abiotic interactions, Nat. Clim. Chang., 5, 56 [online] Available from: http://dx.doi.org/10.1038/nclimate2438, 2014.

Tang, J. and Zhuang, Q.: A global sensitivity analysis and Bayesian inference framework for improving the parameter estimation and prediction of a process-based Terrestrial

1155 Ecosystem Model, J. Geophys. Res. Atmos., 114(D15), doi:10.1029/2009JD011724, 2009.
1156 Thiemann, M., Trosset, M., Gupta, H. and Sorooshian, S.: Bayesian recursive parameter estimation
1157 for hydrologic models, Water Resour. Res., 37(10), 2521–2535,
1158 doi:10.1029/2000WR900405, 2001.
1159 Thyer, M., Renard, B., Kavetski, D., Kuczera, G., Franks, S. W. and Srikanthan, S.: Critical
1160 evaluation of parameter consistency and predictive uncertainty in hydrological modeling:
1161 A case study using Bayesian total error analysis, Water Resour. Res., 45(12), 1–22,
1162 doi:10.1029/2008WR006825, 2009.
1163 Tiedeman, C. R. and Green, C. T.: Effect of correlated observation error on parameters,
1164 predictions, and uncertainty, Water Resour. Res., 49(10), 6339–6355,
1165 doi:10.1002/wrcr.20499, 2013.
1166 Tsai, F. T.-C. and Elshall, A. S.: Hierarchical Bayesian model averaging for hydrostratigraphic
1167 modeling: Uncertainty segregation and comparative evaluation, Water Resour. Res., 49(9),
1168 doi:10.1002/wrcr.20428, 2013.
1169 Tucker, C. L., Bell, J., Pendall, E. and Ogle, K.: Does declining carbon-use efficiency explain
1170 thermal acclimation of soil respiration with warming ?, Glob. Chang. Biol., 252–263,
1171 doi:10.1111/gcb.12036, 2013.
1172 Tucker, C. L., Young, J. M., Williams, D. G. and Ogle, K.: Process-based isotope partitioning of
1173 winter soil respiration in a subalpine ecosystem reveals importance of rhizospheric
1174 respiration, Biogeochemistry, 121, 389–408 [online] Available from:
1175 http://www.jstor.org/stable/24717586, 2014.
1176 Tuomi, M., Vanhala, P., Karhu, K., Fritze, H. and Liski, J.: Heterotrophic soil respiration-
1177 Comparison of different models describing its temperature dependence, Ecol. Modell.,

211(1–2), 182–190, doi:10.1016/j.ecolmodel.2007.09.003, 2008.

Vargas, R., Carbone, M. S., Reichstein, M. and Baldocchi, D. D.: Frontiers and challenges in soil respiration research: from measurements to model-data integration, Biogeochemistry, 102(1), 1–13, doi:10.1007/s10533-010-9462-1, 2011.

Vrugt, J. A. and Ter Braak, C. J. F.: DREAM(D): An adaptive Markov Chain Monte Carlo simulation algorithm to solve discrete, noncontinuous, and combinatorial posterior parameter estimation problems, Hydrol. Earth Syst. Sci., 15(12), 3701–3713, doi:10.5194/hess-15-3701-2011, 2011.

Vrugt, J. A., ter Braak, C. J. F., Diks, C. G. H. and Schoups, G.: Hydrologic data assimilation using particle Markov chain Monte Carlo simulation: Theory, concepts and applications, Adv. Water Resour., 51, 457–478, doi:10.1016/j.advwatres.2012.04.002, 2013.

Wang, G., Post, W. M. and Mayes, M. A.: Development of microbial-enzyme-mediated decomposition model parameters through steady-state and dynamic analyses, Ecol. Appl., 23(1), 255–272, doi:10.1890/12-0681.1, 2013.

Weijs, S. V., Schoups, G. and Van De Giesen, N.: Why hydrological predictions should be evaluated using information theory, Hydrol. Earth Syst. Sci., 14(12), 2545–2558, doi:10.5194/hess-14-2545-2010, 2010.

Westerberg, I. K., Guerrero, J. L., Younger, P. M., Beven, K. J., Seibert, J., Halldin, S., Freer, J. E. and Xu, C. Y.: Calibration of hydrological models using flow-duration curves, Hydrol. Earth Syst. Sci., 15(7), 2205–2227, doi:10.5194/hess-15-2205-2011, 2011.

Wieder, W. R., Bonan, G. B. and Allison, S. D.: Global soil carbon projections are improved by modelling microbial processes, Nat. Clim. Chang., 3, 909 [online] Available from: http://dx.doi.org/10.1038/nclimate1951, 2013.

1201 Wieder, W. R., Allison, S. D., Davidson, E. A., Georgiou, K., Hararuk, O., He, Y., Hopkins, F.,
1202 Luo, Y., Smith, M. J., Sulman, B., Todd-Brown, K., Wang, Y.-P., Xia, J. and Xu, X.:
1203 Explicitly representing soil microbial processes in Earth system models, Global
1204 Biogeochem. Cycles, 29(10), 1782–1800, doi:10.1002/2015GB005188, 2015.
1205 Van Wijk, M. T., Van Putten, B., Hollinger, D. Y. and Richardson, A. D.: Comparison of different
1206 objective functions for parameterization of simple respiration models, J. Geophys. Res.
1207 Biogeosciences, 113(3), 1–11, doi:10.1029/2007JG000643, 2008.
1208 Xu, T., White, L., Hui, D. and Luo, Y.: Probabilistic inversion of a terrestrial ecosystem model:
1209 Analysis of uncertainty in parameter estimation and model prediction, Global Biogeochem.
1210 Cycles, 20(2), 1–15, doi:10.1029/2005GB002468, 2006.
1211 Xu, X., Schimel, J. P., Thornton, P. E., Song, X., Yuan, F. and Goswami, S.: Substrate and
1212 environmental controls on microbial assimilation of soil organic carbon: a framework for
1213 Earth system models, Ecol. Lett., 17(5), 547–555, doi:10.1111/ele.12254, 2014.
1214 Yeluripati, J. B., van Oijen, M., Wattenbach, M., Neftel, A., Ammann, A., Parton, W. J. and Smith,
1215 P.: Bayesian calibration as a tool for initialising the carbon pools of dynamic soil models,
1216 Soil Biol. Biochem., 41(12), 2579–2583, doi:10.1016/j.soilbio.2009.08.021, 2009.
1217 Yuan, W., Liang, S., Liu, S., Weng, E., Luo, Y. and Hollinger, D.: Improving model parameter
1218 estimation using coupling relationships between vegetation production and ecosystem
1219 respiration, Ecol. Modell., 240, 29–40, doi:10.1016/j.ecolmodel.2012.04.027, 2012.
1220 Yuan, W., Xu, W., Ma, M., Chen, S. and Liu, W.: Agricultural and Forest Meteorology Improved
1221 snow cover model in terrestrial ecosystem models over the Qinghai – Tibetan Plateau,
1222 Agric. For. Meteorol., 218–219, 161–170, doi:10.1016/j.agrformet.2015.12.004, 2016.
1223 Zhang, X., Niu, G.-Y., Elshall, A. S., Ye, M., Barron-Gafford, G. A. and Pavao-Zuckerman, M.:

1224 Assessing five evolving microbial enzyme models against field measurements from a
1225 semiarid savannah - What are the mechanisms of soil respiration pulses?, Geophys. Res.
1226 Lett., 41(18), doi:10.1002/2014GL061399, 2014.
1227 Zhou, X., Luo, Y., Gao, C., Verburg, P. S. J., Arnone, J. A., Darrouzet-Nardi, A. and Schimel, D.
1228 S.: Concurrent and lagged impacts of an anomalously warm year on autotrophic and
1229 heterotrophic components of soil respiration: A deconvolution analysis, New Phytol.,
1230 187(1), 184–198, doi:10.1111/j.1469-8137.2010.03256.x, 2010.
1231

Figure 1. Diagram of model 6C representing the processes of (1) degradation of soil organic carbon (SOC) to dissolved organic carbon (DOC) through catalysis of enzymes (ENZ) produced by microbes (MIC), (2) MIC uptake of DOC, and (3) microbial (MIC) respiration to produce $CO_2$ (CUE is the carbon use efficiency). SOC degradation and microbial uptake rates are controlled by water saturation ($\theta / \theta_s$). The DOC and ENZ pools are split into two subpools, one for the wet zone and the other for the dry zone of the soil pore space. Microbial uptake of DOC occurs only in the wet zone, and the uptake rate is linearly related to $\theta/\theta_s$. Catalysis through ENZ in the wet zone is proportional to $\theta/\theta_s$, while that in the dry zone is proportional to $1 - \theta/\theta_s$. $V_{max}$ ($s^{-1}$) is the maximum rate, and $K_m$ is the half-saturation concentration.

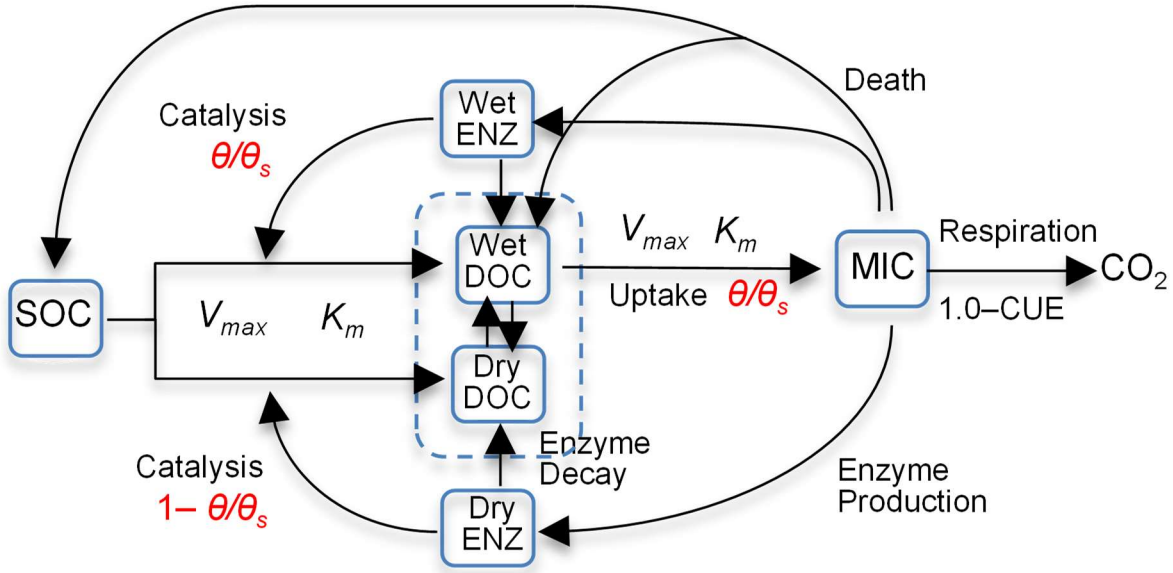

Figure 2. Time series of soil moisture and efflux observations. The dashed line marks the divide of the dataset into calibration and validation periods.

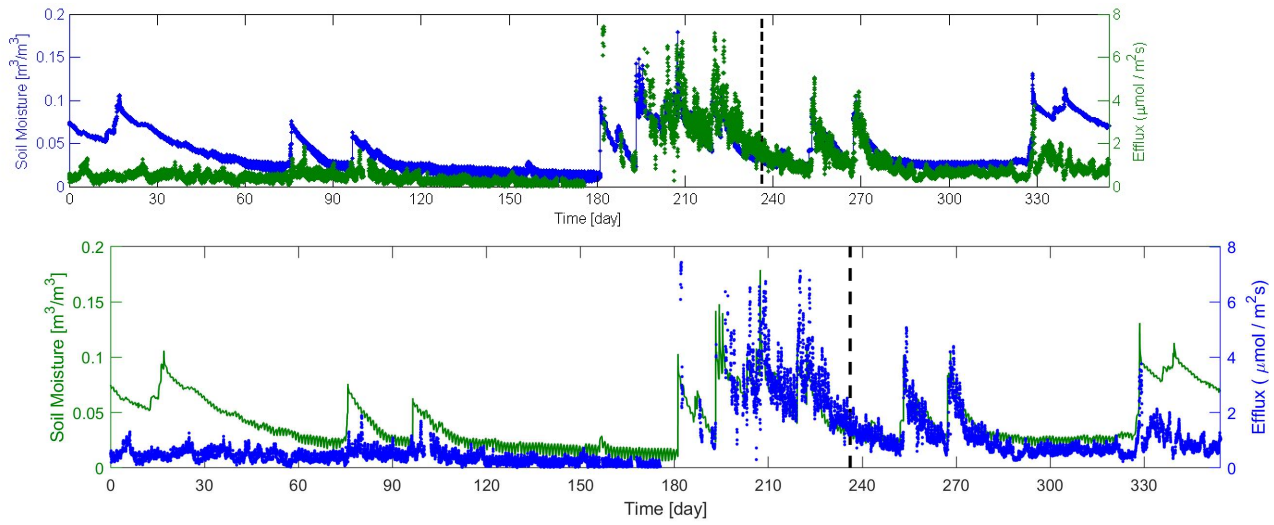

Figure 3. Residual analysis of the best realization (among multiple MCMC realizations) for model 6C using data models (a-c) SLS and (d-f) WSEP-AC.

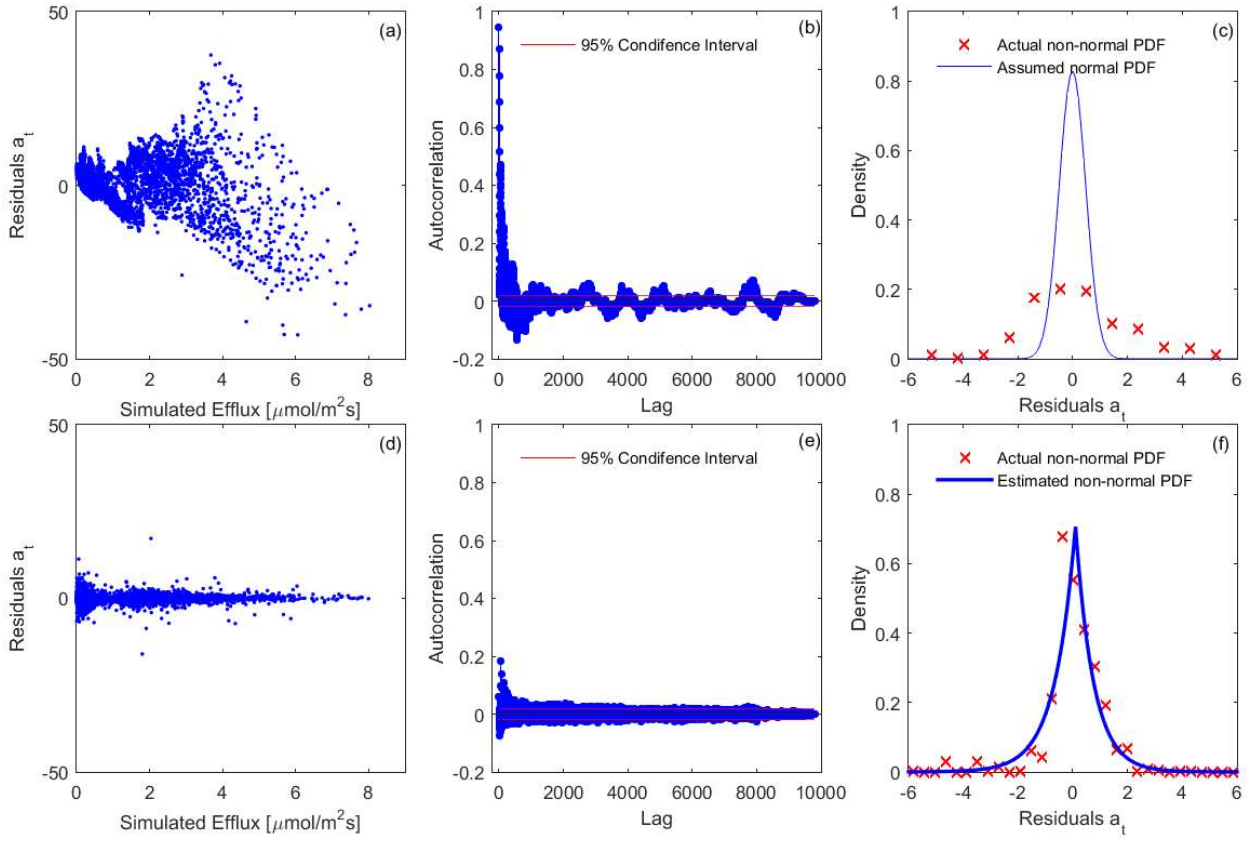

Figure 4. Residual quantile-quantile (Q-Q) plots of the best realization (among multiple MCMC realizations) for the three soil respiration models and eight data models.

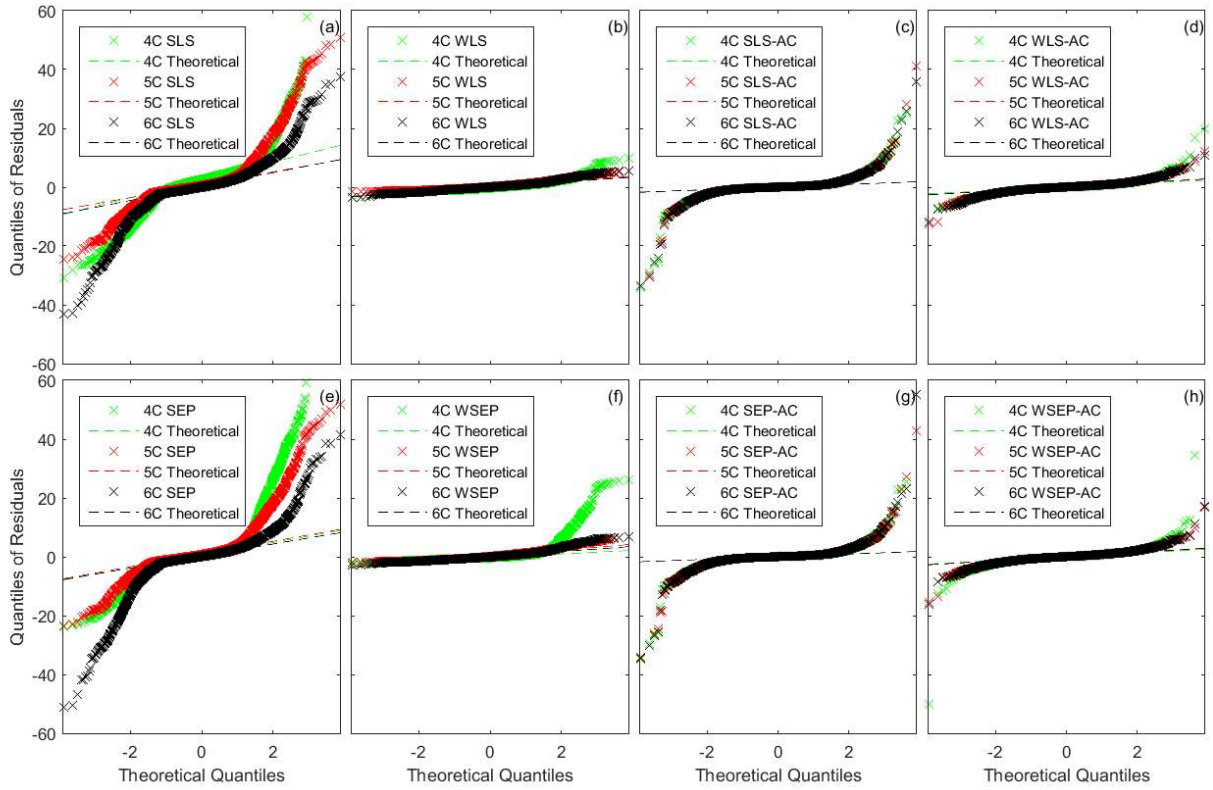

1259 Figure 5. Marginal posterior parameter density of carbon use efficiency (CUE) for the three soil
1260 respiration models and eight data models.
1261

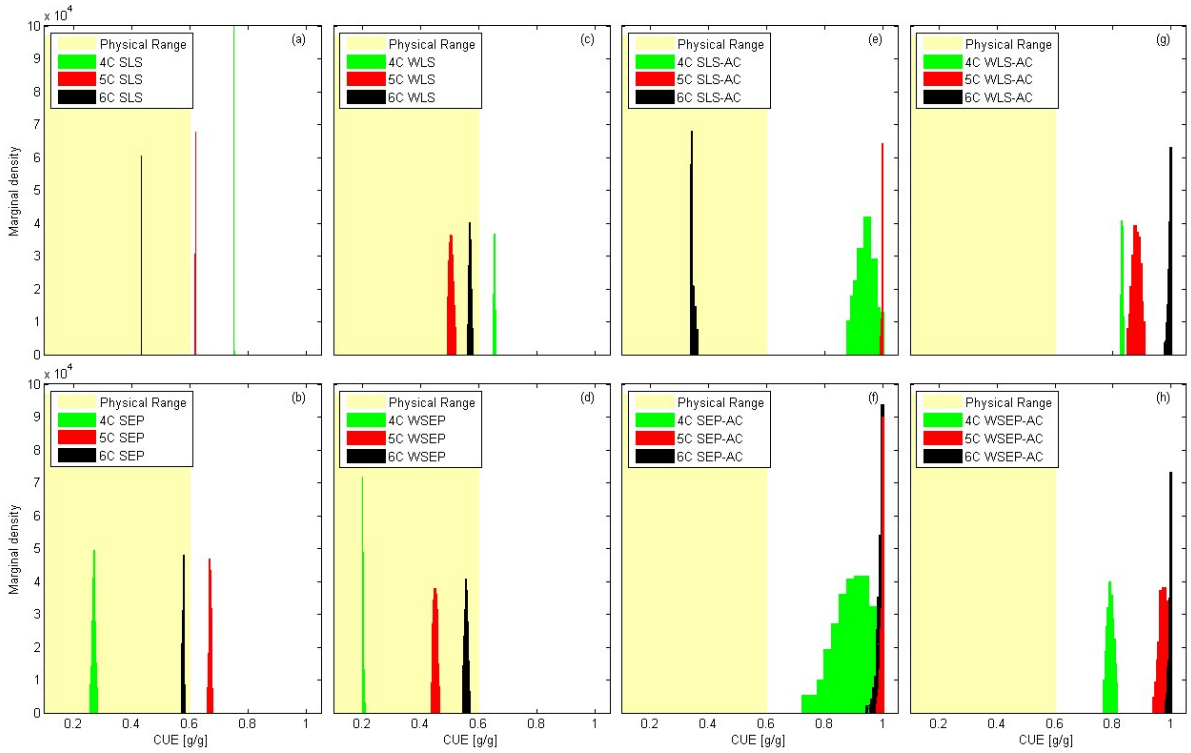


1262

Figure 6. Observation data (blue dots) and mean prediction (green line) and 95% credible intervals (red line) of prediction ensembles for (a)-(f) the calibration period and (g)-(l) the validation period. The plots are for the three soil respiration models using data models SLS and WSEP-AC. *The prediction ensembles are generated to consider parametric uncertainty of the soil respiration models only.*

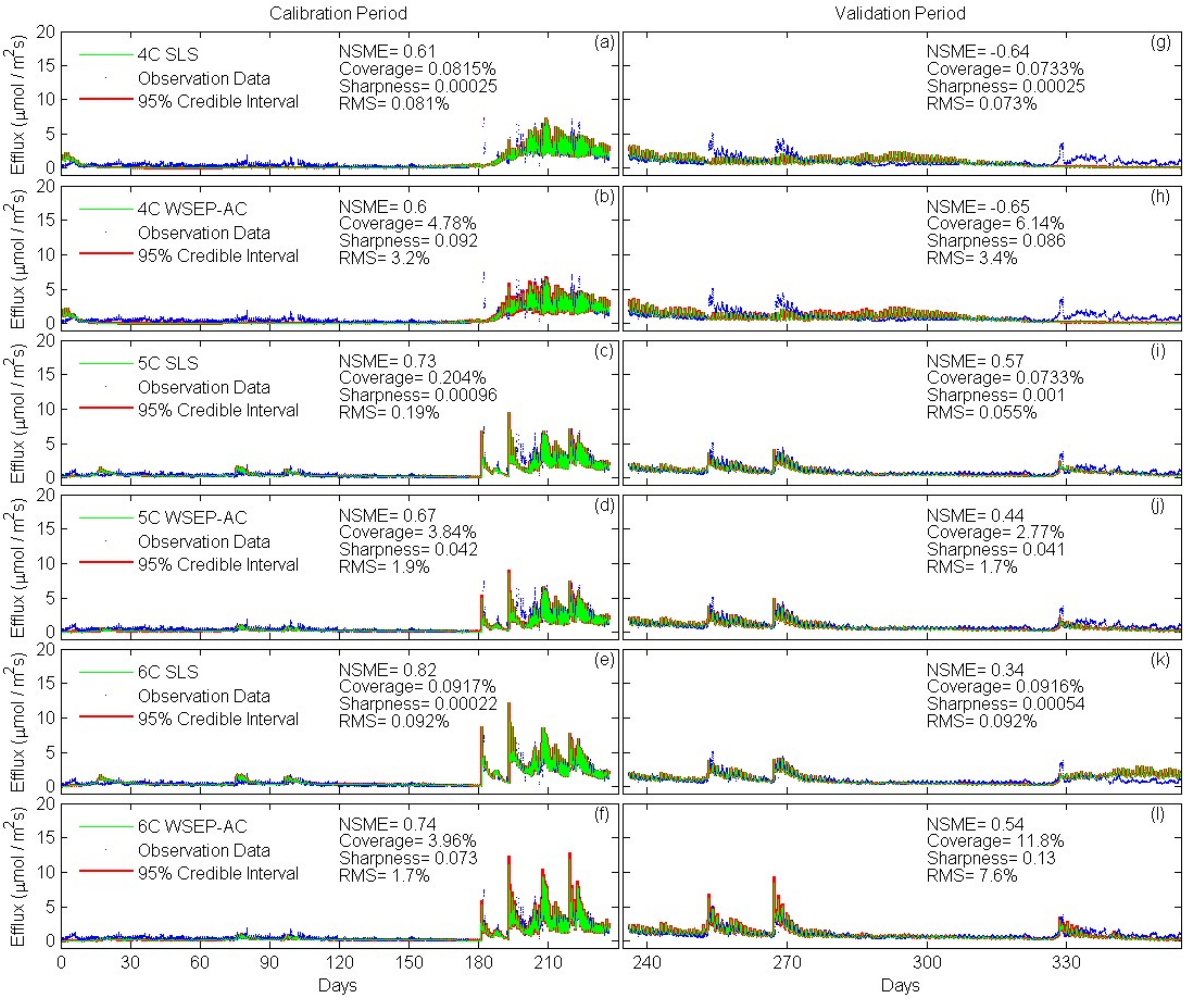

Figure 7. (a-b) Nash-Sutcliffe model efficiency (NSME), (c)-(d) sharpness, (e)-(f) predictive coverage, and (g)-(h) relative model score for measuring predictive performance of the three soil respiration models and the eight data models during the calibration and cross-validation periods. *The statistics are evaluated from the prediction ensembles generated to consider parametric uncertainty of the soil respiration models only.*

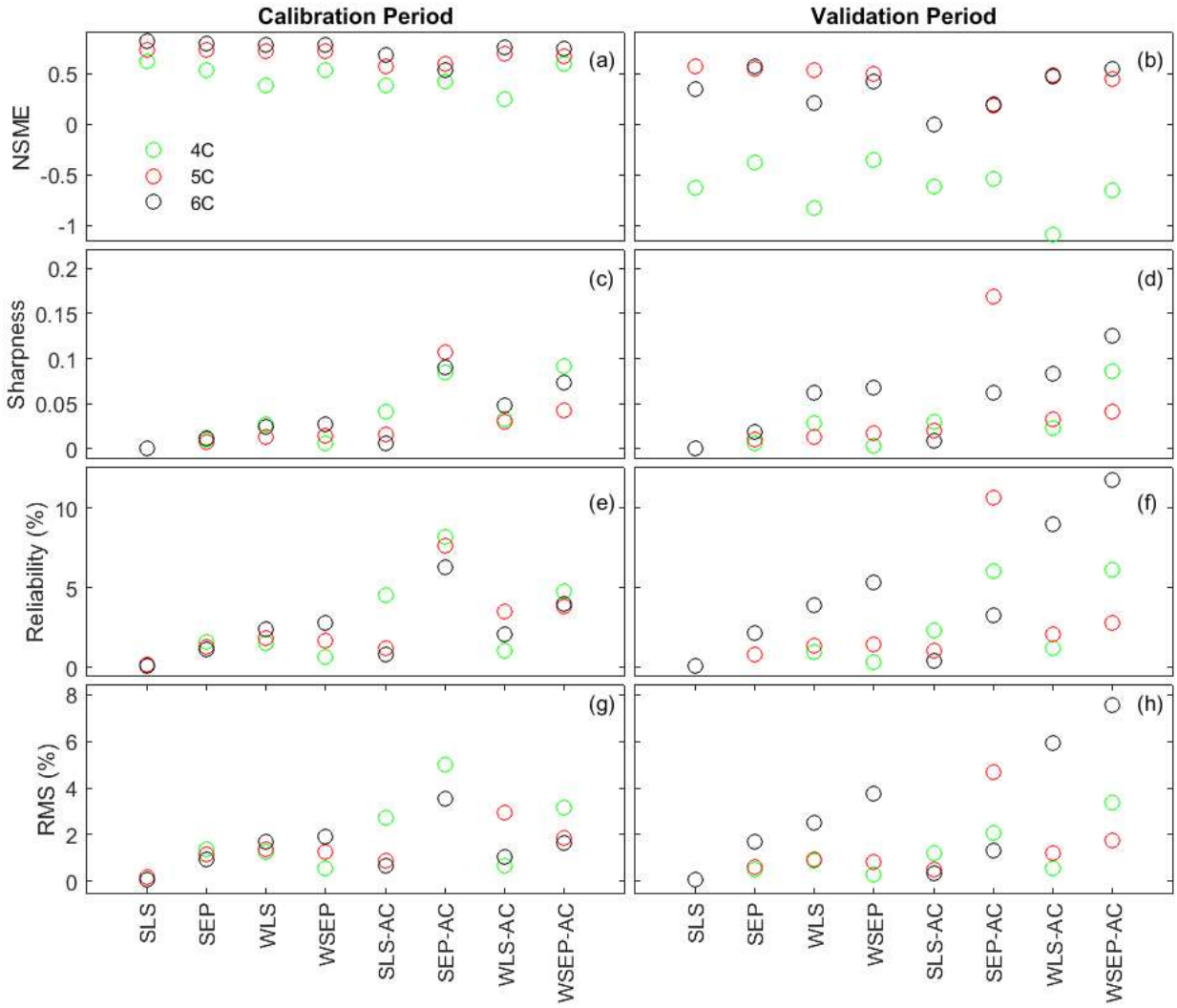

Figure 8. Observation data (blue dots) and mean prediction (green line) and 95% credible intervals (red line) of prediction ensembles for (a)-(f) the calibration period and (g)-(l) the validation period. The plots are for the three soil respiration models using data models SLS and WSEP-AC. *The prediction ensembles are generated to consider parametric uncertainty of not only the soil respiration models but also the data models.*

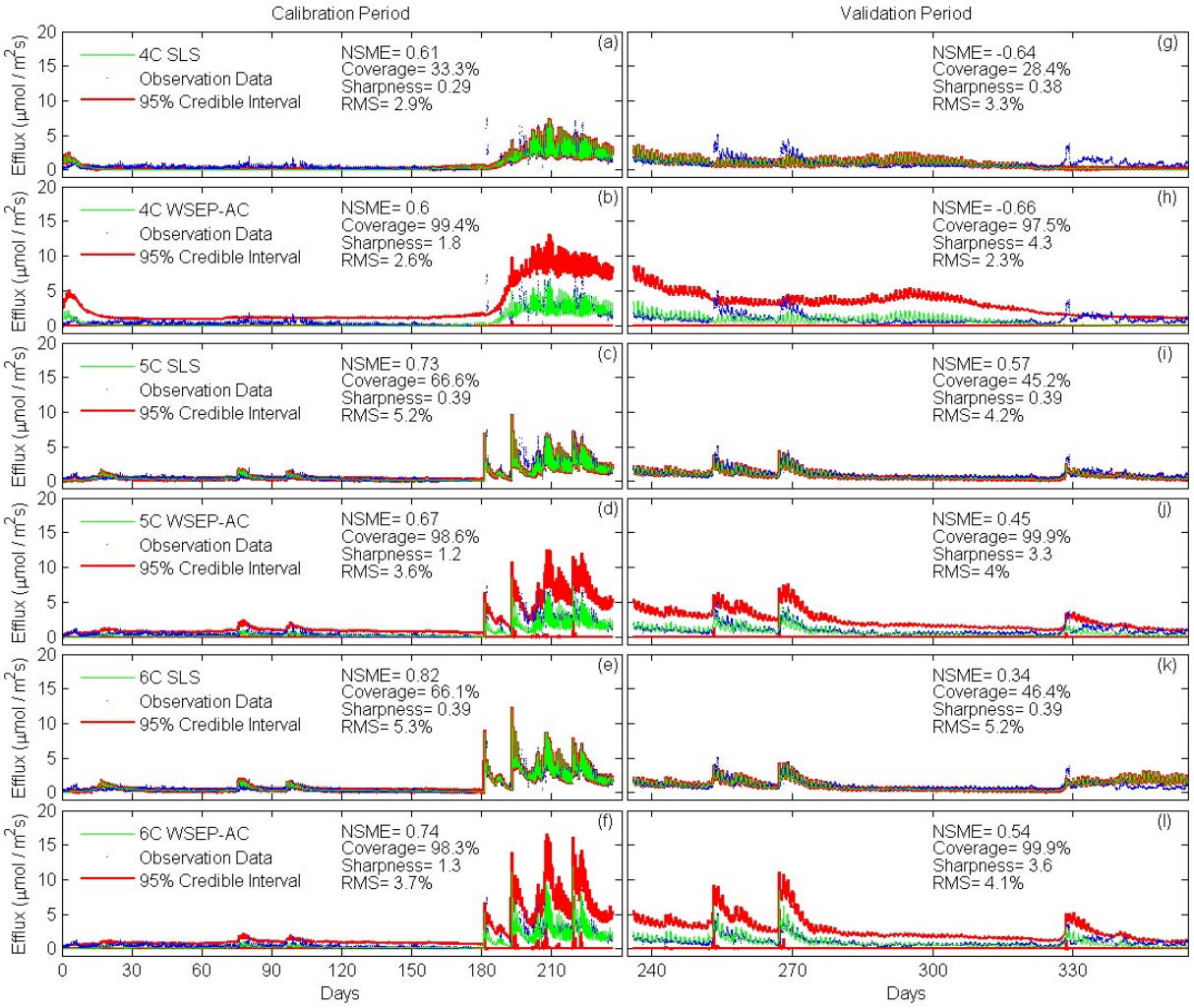

Figure 9. (a-b) Nash-Sutcliffe model efficiency (NSME), (c)-(d) sharpness, (e)-(f) predictive coverage, and (g)-(h) relative model score for measuring predictive performance of the three soil respiration models and the eight data models during the calibration and cross-validation periods. *The statistics are evaluated from the prediction ensembles generated to consider parametric uncertainty of not only the soil respiration models but also the data models.*

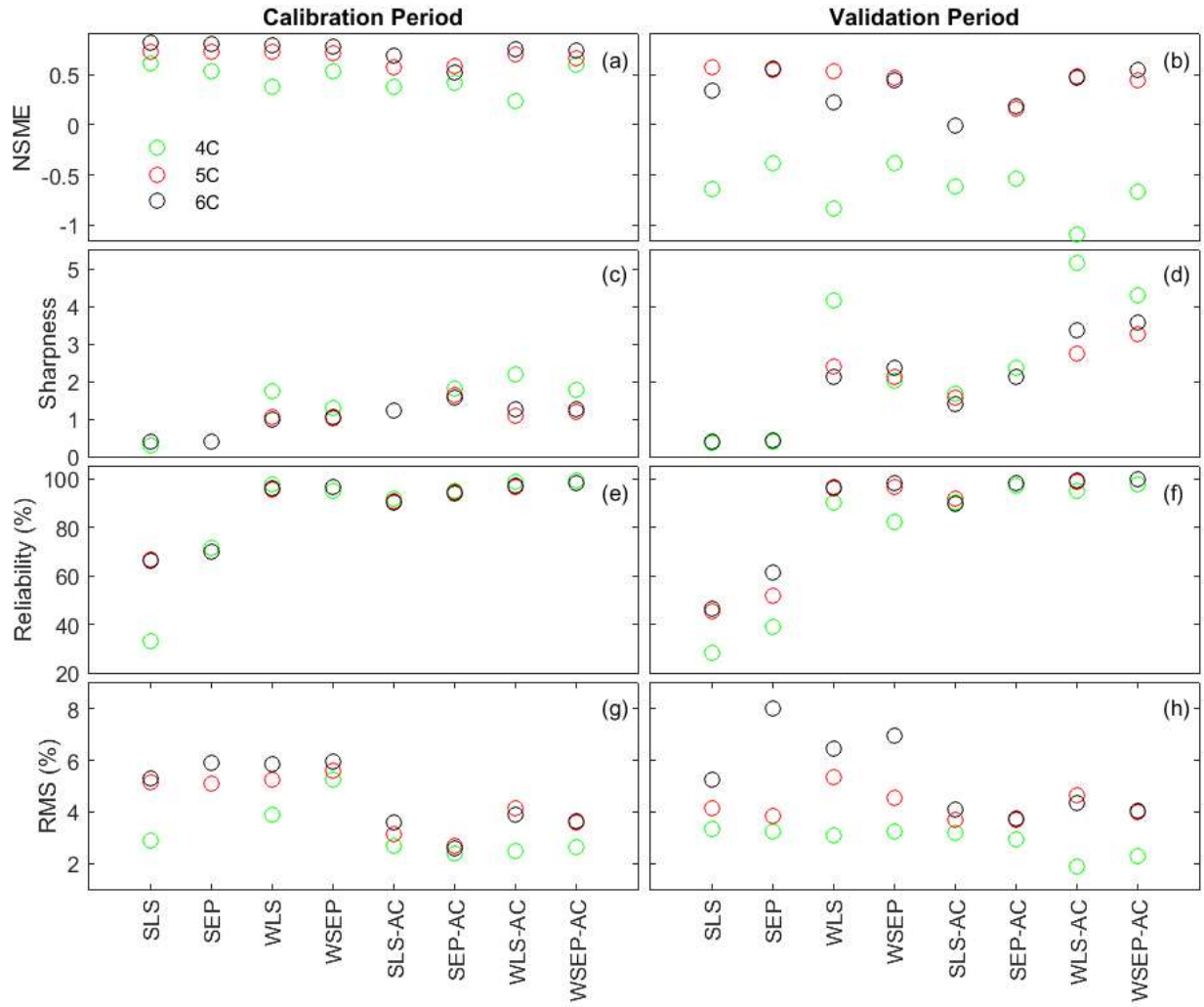

Figure 10. Observation data (blue dots) and mean prediction (green line) and 95% credible intervals (red line) for 6C for the eight likelihood functions during the calibration period (a)-(h) and the validation period (i)-(p). *The prediction ensembles are generated to consider parametric uncertainty of not only the soil respiration models but also the data models.*